



A novel passive sampling and sequential extraction approach to investigate desorption kinetics of emerging organic contaminants at the sediment–water interface

Xiaowen Ji^{a,b}, Jonathan K. Challis^c, Jenna Cantin^c, Ana S. Cardenas Perez^a, Yufeng Gong^c, John P. Giesy^{c,d,e}, Markus Brinkmann^{a,b,c,f,*}

^a School of Environment and Sustainability, University of Saskatchewan, Saskatoon, Canada

^b Global Institute for Water Security, University of Saskatchewan, Saskatoon, Canada

^c Toxicology Centre, University of Saskatchewan, Saskatoon, Canada

^d Department of Veterinary Biomedical Sciences, University of Saskatchewan, Saskatoon, Canada

^e Department of Environmental Sciences, Baylor University, Waco, Texas, USA

^f Centre for Hydrology, University of Saskatchewan, Saskatoon, Canada

ARTICLE INFO

Keywords:

DGT, DIFS model
Desorption kinetics
Antipsychotic drugs
Sediment
Adsorbing fractions

ABSTRACT

Forms of organic contaminants is an important driver of bioavailable fraction and desorption kinetics of pollutants binding to sediments. To determine fluxes and resupply of nine environmentally-relevant antipsychotic drugs, which are emerging pollutants that can have adverse effects on aquatic organisms, interface passive samplers of diffusive gradients in thin films (DGT) were deployed for 21 days, *in situ* at the sediment–water interface in submerged sandy riverbank sediments. At each deployment time, samples of sediment were collected and subjected to consecutive extraction of pore water, as well as rapidly-desorbing (labile), stable-desorbing, and bound residue fractions. Concentrations of antipsychotic drugs decreased with sediment depth with the greatest concentrations observed in the top 2 cm. Positive fluxes of antipsychotic drugs were observed from sediment to surface water. The dynamic fraction transfer model indicated that the labile fraction can be resupplied with a lag time (> 21 d). When results were further interpreted using the DGT-induced fluxes in soils and sediments (DIFS) model, partial resupply of antipsychotic drugs from sediment particles to porewater was demonstrated. Desorption occurred within the entirety of the observed 15 cm depth of sediment. Fastest rates of resupply were found for carbamazepine and lamotrigine. Size of the labile pool estimated by the DIFS model did not fully explain the observed resupply, while a first-order three-compartment kinetic model for the fast-desorbing fraction can be used to supplement DIFS predictions with estimations of labile pool size.

1. Introduction

In aquatic ecosystems, sediments can act as both sinks and sources of pollutants. Some micropollutants are transported in the water column adsorbed to organic particles, which will ultimately be deposited during periods of lesser flow to bottom sediments (Megahan, 1999). Some organic pollutants sequestered in sediments are not prone to rapid biodegradation and can be accumulated into benthic organisms (Zhao et al., 2009).

Fates of organic compounds deposited in sediments depends on their net fluxes at the sediment–water interface. Fractions of organic compounds desorbed from sediment to water are largely controlled by

processes of exchange between aqueous and solid phases within sediment (Bondarenko and Gan, 2004). An advective flux can be induced when concentrations of compounds in the solution phase are depleted and a resupply to the solution phase occurs from the adsorbed fraction. This is based on the capacity of remobilization and the rate of desorption of chemicals from the solid phase. Generally, fluxes via molecular diffusion, is driven by the concentration gradient between sediment porewater and overlying bulk water through a diffusion-limiting boundary layer, which is formed at the sediment–water interface (Eek et al., 2010). The flux can be estimated by use of passive sampling approaches that can pre-concentrate trace chemicals through non-disruptive *in situ* sampling (Alvarez et al., 2004).

* Corresponding author.

E-mail address: markus.brinkmann@usask.ca (M. Brinkmann).

<https://doi.org/10.1016/j.watres.2022.118455>

Received 9 February 2022; Received in revised form 27 March 2022; Accepted 11 April 2022

Available online 13 April 2022

0043-1354/© 2022 Elsevier Ltd. All rights reserved.

A recently developed diffusive gradient in thin-films (DGT) technique is able to measure freely dissolved compounds (Fernandez et al., 2009) and has been used for investigating organic contaminants in sediments (Li et al., 2021; Mechelke et al., 2019). DGT can be used as a dynamic tool for measuring labile concentrations, which are fractions of chemicals that can be easily dissociated and resupplied to the porewater and its resupply capacity from the solid phase (Iuele et al., 2021). A numerical model, known as DGT-induced fluxes in soil and sediments (DIFS) which can be formulated in various dimensionalities (1D/2D/3D-DIFS) (Harper et al., 2000; Sochaczewski et al., 2007), was developed to simulate DGT adsorption and describe analyte resupply kinetics from solid phases. The DIFS model was first applied to quantify desorption kinetics and labile pools of pesticides in intact sediment cores in the laboratory-controlled conditions (Li et al. (2021)). However, other influences, such as resuspension/desorption (Eek et al., 2010) and bio-irrigation, by suction of overlaying water by benthic organisms through their burrows (Benoit et al., 2009) can affect the observed net fluxes.

Because sediment can be a heterogeneous matrix, organic pollutants can exist in various fractions, which can influence kinetics of desorption. It has been reported that partitioning influences distributions of organic pollutants in sediments (Demars et al., 1995; He et al., 2016). Although most studies considered the distribution of pollutants between solid fractions and interstitial water within sediments, the binding mechanisms and intensities established between particles and pollutants can be complex (Demars et al., 1995). Three fractions of organic pollutants in sediments have been widely recognized: (i) the fast-desorbing fraction is weakly and reversibly bound to sediments and can rapidly desorb into the interstitial water (Semple et al., 2004); (ii) the stable-desorbing fraction can be described as a reversibly bound but slow-desorbing fraction (Schwab and Brack, 2007); and (iii) the non-extractable phase, which is covalently bound to or sequestered by organic matter in sediments (Schäffer et al., 2018) and has been defined as “bound residues” by the International Union of Pure and Applied Chemistry (Roberts, 1984).

When xenobiotics enter sediments, they can undergo transfer as well due to the wide range of structural units and functional groups present in organic macromolecules (Hayes and Swift, 1978). Therefore, organic pollutants can be stored as bound-residue form in sediments where they might not appear to be hazardous in the short term, but might be released when a sudden alternations of environment occur (Supplementary Material Supplementary Fig. S1). This phenomenon has been defined as a ‘chemical time bomb’ (Stigliani, 1991). This fraction of organic pollutants can be a potential source for re-supply to the aqueous phase. However, to date, there are no *in situ* studies of kinetics of desorption in sediments, that have considered these three fractions. The current DIFS model only considers the single labile pool size that is based on initial sediment solution concentration (Menezes-Blackburn et al., 2019). However, resupply to the labile pool needs to consider rates of transfer between various binding forms and equilibrium of labile analytes reached by a kinetic model, which might provide additional information on kinetic processes in sediments and help describe the flux between sediment and water in aquatic systems.

To address these uncertainties and resolve gaps in data, the objectives of this study were to: (i) obtain time-resolved field measurements for nine selected antipsychotic pharmaceuticals; (ii) study the sorption phase for these compounds from water to sediments using DGT devices; (iii) investigate and model desorption rates from the fractions—transfer in sediments and compare measurements to values predicted by the DIFS model.

2. Materials and methods

2.1. Chemicals

Nine high purity (> 98%) antipsychotic drugs, amitriptyline, bupropion, carbamazepine, citalopram, clozapine, duloxetine,

fluoxetine, lamotrigine and venlafaxine, and the corresponding nine stable isotope-labeled internal standards, i.e., amitriptyline- d_6 , bupropion- d_9 , carbamazepine- d_{10} , citalopram- d_6 , clozapine- d_4 , duloxetine- d_7 , fluoxetine- d_5 , lamotrigine- $[^{13}C,^{15}N_4]$, and venlafaxine- d_6 , were used (Table S1 and Section S1).

2.2. Assembly of DGT devices

A standard size of polytetrafluoroethylene (PTFE) DGT device with 0.75 mm Septra™-ZT (surface modified styrene divinylbenzene, Phenomenex, Torrance, CA) binding gels (~25 mg per gel), 0.75 mm agarose diffusive gels, and a 0.45 μ m pore size polyethersulfone (PES) filter membrane (Sartorius Stedim Biotech GmbH, Göttingen, Germany) were prepared as previously described (Challis et al., 2016). A DGT sediment probe (length: 170 mm and width: 40 mm, Supplementary Fig. S2) was constructed from acrylonitrile butadiene styrene (ABS) polymer and contained the same three layers as the standard DGT device, with different dimensions of binding gel (~250 mg per gel), diffusive gel, and PES membrane (length: 150.3 mm and width: 20.4 mm). Results of adsorption tests with DGT moulding, agarose gel, PES membrane, and binding gel are provided in Section S2.

2.3. Background of sampling site

The deployment and sampling site (52°19′10.8″N 106°27′34.3″W; Clarkboro Ferry, South Saskatchewan River, Saskatoon; Supplementary Fig. S3a) was selected because it is ~20 km downstream of the City of Saskatoon’s wastewater treatment plant and in close proximity of the laboratory so that DGT devices and samples can be obtained and transported quickly. The nine selected antipsychotic drugs were found in water, sediments, and fish of this site during previous investigations (unpublished data).

The sampling site is in the prairie physiographic region, which is characterized by rich soil, thick glacial drift, and extensive aquifer systems. To avoid fluxes of chemicals from groundwater and significant runoff from the surrounding land surface, the deployment site (Supplementary Fig. S3b) was selected to be located in the riverbank (depth < 1 m) with a stable deposited layer on 1st September 2021 (the physicochemical properties of sediment are shown in Table S2).

2.4. DGT field deployment and sediment sampling

In the field, one DGT probe was attached in the bottom, and three DGT samplers were attached above the DGT probe, on perforated stainless steel profiles (thickness: 3.18 cm, width: 3.18 cm, length: 183 cm). Three separate profiles with attached samplers were slowly inserted into sediments, with 2 cm of the probe board exposed out of sediments (15 cm was put into the sediment), and were supported by three cement blocks (height: 19 cm, width: 27 cm) for protection (the setup is presented in Fig. 1). DGT devices were deployed and replaced after 1, 3, 6, 9, 12, 15, and 21 d. Meanwhile, three sediment cores adjacent to the DGT probes were sampled using a PVC sampling tube (length: 15 cm, diameter: 2 cm). One additional sample of sediment was taken by use of a small shovel for the determination of matrix effects on extraction and concentration recoveries.

Once the DGT devices were retrieved, remaining sediment particles on probes and samplers were washed away using Milli-Q water, placed into sealed bags, and wrapped with aluminum foil. Sediment cores were stored in a cooler with ice bags. After installation of new DGT devices, retrieved DGT devices and sampled sediments were immediately transported to the laboratory (Toxicology center, University of Saskatchewan), where the binding gels were carefully removed and placed into amber glass vials. Wet sediment cores were immediately drained for 2 h to determine maximum water holding capacity (Priha and Smolander, 1999). Then, sediment cores were sliced into 2 cm-intervals, and each slice was centrifuged at 1280 \times g for 40 min to obtain sediment

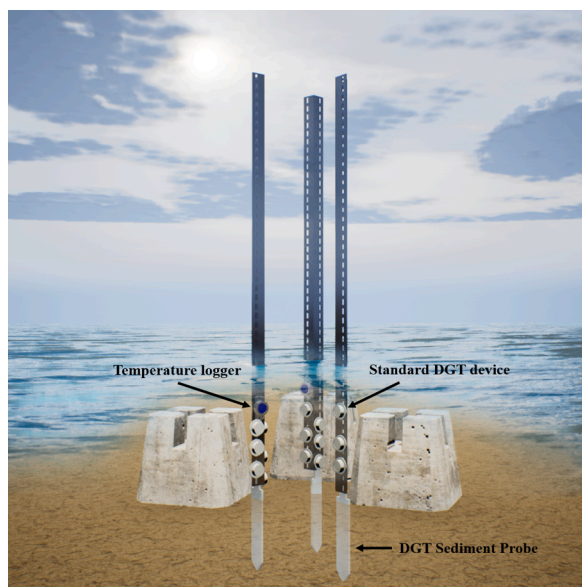


Fig. 1. The three-dimensional simulation of the setup for fixation of DGT sediment probes and standard DGT samplers. The blue circular attachments are bluetooth-controlled temperature loggers.

porewater that was filtered through a $0.20\ \mu\text{m}$ membrane filter (13 mm diameter, Millex-GN Nylon membrane, hydrophilic, MilliporeSigma, Oakville, ON) and then concentrated by solid-phase extraction (Strata-X SPE cartridge, details in Section S3). The binding gel was removed by use of a round spatula from the standard DGT device. The binding gel of the DGT sediment probe was sliced at 2 cm intervals using a razor blade (pre-rinsed by methanol). All binding gels were transferred to 30-mL amber glass vials.

2.5. Extraction

2.5.1. DGT binding gel

Fifty nanograms of internal standards were added to the binding gel. Five milliliters of methanol were added into the vial for ultrasonic extraction for 10 min, for a total of three times. Extracts were combined and concentrated to dryness with a gentle flow of nitrogen gas, reconstituted in 1 mL of methanol, and filtered through Target2™ $0.2\ \mu\text{m}$

PTFE syringe filters (Thermo Scientific, Waltham, MA) into 2-mL LC vials.

2.5.2. Sediment

After collecting the porewater, sediments were transferred to a freezer ($-20\ ^\circ\text{C}$) for 24 h and lyophilized (Dura-Dry MP FD2085, Stone Ridge, NY). The triplicates of a 5-g aliquot of sediment at different sampling times were transferred to Lysing matrix E 50 mL tubes (Fisher Scientific) for sequential extraction (Fig. 2). The fast-desorbing fraction, stable-desorbing fraction, and bound-residue fraction of antipsychotic drugs (Log Kow = 0.99–4.95, Table S1) were sequentially extracted using (1) methanol, (2) a mixture of methanol and dichloromethane (1:1, v:v) with ultrasound, and (3) alkaline hydrolysis at $80\ ^\circ\text{C}$, respectively.

2.5.2.1. Fast-desorbing fraction. The fast-desorbing fraction is defined as a consecutive desorption with time, which can be represented by single-point extraction methods (Muijs and Jonker, 2011). A single-point extraction by methanol was used in this study, and extraction time was determined by a consecutive extraction using a first-order three-compartment kinetic model (details shown in Section S4). In order to conduct consecutive extraction, 5 g of lyophilized sediment were extracted using 5 mL methanol in a shaker (1500 rpm, Heidolph™ Multi Reax Vortex Mixer, Fisher Scientific). Five milligrams of sodium azide was added for inhibition of microbial activity (Skipper et al., 1996). At the time interval of 0.2, 0.4, 0.6, 1, 3, 10, 24, 48, 96, and 250 h, the samples were centrifuged, and the methanol sampled and refreshed. The sampled methanol was passed through a $0.2\ \mu\text{m}$ PTFE membrane filter after addition of internal standards and concentrated to 1 mL for instrumental analysis.

2.5.2.2. Stable desorbing fraction. The stable desorbing fractions of antipsychotic drugs were extracted three times with 10 mL methanol: dichloromethane (1:1, v/v) with ultrasound (Fig. 2). After centrifugation, the combined extracts were passed through a $0.2\ \mu\text{m}$ PTFE membrane filter, followed by SPE concentration procedure (Section S3) before instrumental analysis.

2.5.2.3. Bound-residue fraction. Alkaline hydrolysis has been widely used for the dissolution of organic matter, which in turn releases non-extractable organic pollutants, which are sequestered or occluded with organic matter in soils and sediments. This method was adopted in the present study to extract the bound-residue fraction of antipsychotic



Fig. 2. Process diagram of the sequential extraction procedure to obtain rapidly-desorbing, stable desorbing, and bound residue fractions of lyophilized sediments after separation of porewater.

drugs in sediments. Residual sediments from previous ultrasonic extractions were added to 5 mL of 1 M NaOH solution and then heated at 80 °C for 8 h. After cooling, the samples were lyophilized and extracted using the same procedure as the stable desorbing fraction. In order to test whether high temperature or hydrolysis would influence the analytes, the mixture of nine antipsychotic drugs was spiked in 10 mL of 1 M NaOH solutions to reach the concentration of 1, 10, and 100 $\mu\text{g L}^{-1}$, and heated at 80 °C for 8 h. After cooling, the solutions were processed following the previously described SPE procedure.

2.6. Determination of agarose diffusion coefficient

To determine efficiency for deriving diffusion coefficients (D) for the nine analytes, two major methods were compared: the diffusion cell method (Westrin et al., 1994) and the slice stacking method (Rusina et al., 2010). Both methods were conducted in an environmental chamber at a temperature of 25 °C. The diffusion coefficient of analytes in water (D_w) was further estimated by the Hayduk-Laudie equation (Hayduk and Laudie, 1974).

The diffusion cell method is based on the analytes passing through a membrane from one water cell to another (Supplementary Fig. S4a). Each cell (made of clear acrylic) held ca. 50 mL and had a 2.3 cm^2 circular connecting window. A diffusive gel was placed on the window (a spacer was made based on the gel thickness) between the two cells and gently sealed together with clamps. Each cell had a total volume of 40 mL. To each cell, 20 mL of 10 mM NaCl was added, followed by a spike of the 9-analyte stock mixture (1000 $\mu\text{g L}^{-1}$) prepared in 5% methanol into the source cell at a target concentration of 500 $\mu\text{g L}^{-1}$. Meanwhile, 20 mL of 5% methanol spike was added to the receiving cell. Both cells were stirred gently on stir-plates. Triplicate samples (200 μL) were taken from the receiving cell and source cell at ten different time points spread out over the experimental duration (5 to 140 min). Samples were pipetted directly into LC vials and before instrumental analysis. External standardization was applied for these experiments due to no extraction processes.

The slice stacking method is based on analytes diffusing through several layers of gels (Supplementary Fig. S4b). Sixteen agarose gels were spiked by immersing them in 50 mL spiked at a concentration of 500 $\mu\text{g L}^{-1}$ of the nine antipsychotic drugs for 24 h. Afterwards, 10 spiked gels were removed and capped with 7 unspiked gels on a glass plate wrapped with aluminum foil. The remaining gels were taken as blank for measuring the initial analyte concentrations. The exposure time was selected as 60, 90, and 120 min. After exposure, the stacks were disassembled, and each gel was extracted with the same method of extraction used for binding gels (chapter 2.5.2.1). Calculation of D values for the both methods and different temperature are detailed in Section S5.

2.7. Calculation of DGT-derived parameters

Binding layers in DGT functions as a sink for compounds in the sediment porewater/water, where an induced flux from the sediment/water passes through the diffusive layer and is bound in the binding layer. For sediments, the magnitude of this flux can be measured through interfacial concentration, which is determined by the desorption kinetics between the adsorption of solute induced by the DGT probe and the capability to resupply solute from the sediment solid phase to the probe interface. The time-averaged interfacial concentration of dissolved compounds at each deployment time ($C_{DGT,i}$) can be calculated (Eq. (1)) (Zhang and Davison, 1995).

$$C_{DGT,i} = \frac{M_i \times \delta_{total}}{D_{m,i} \times A_e \times t_i} \quad (1)$$

where M_i is the accumulated mass of analyte in the binding gel at deployment time i (t_i), δ_{total} is the total thickness of the diffusive layer (it

includes the 0.15 mm PES filter membrane and the 0.75 mm agarose diffusive gel), $D_{m,i}$ is the mean temperature-adapted diffusion coefficient of each analyte at each deployment time i , and A_e is the effective exposure window of DGT devices (3.14 cm^2 for standard device and 30.66 cm^2 for DGT probe). An index of the magnitude of depletion of sediment porewater concentration to the device interface, R , is the ratio between $C_{DGT,i}$ and the initial sediment porewater concentration ($C_{p,i}$) at each deployment time i (Eq. (2)).

$$R = \frac{C_{DGT,i}}{C_{p,i}} \quad (2)$$

In most common cases in the real aquatic ecosystem, the R value meets the partial case ($0.1 < R < 0.95$), in which some resupply from the solid phase but inadequate to maintain the initial $C_{p,i}$ (Harper et al., 1998). The calculation of diffusion between sediment and water is shown in Section S6.

2.8. Numerical modeling of DGT deployments using DIFS

The 2D/3D-DIFS model developed by Sochaczewski et al. (2007) simulates DGT-induced fluxes from soil or sediments in consideration of solute diffusion within two dimensions and incorporation of essential model calibrations. Although 2D-DIFS considers the domain as the partial cross-section along the axis perpendicular to the diffusive gel interface, of which the origin is situated at the center, the 2D model was shown to be a good approximation of the full 3D model (Sochaczewski et al., 2007). Therefore, in the study, results of which are presented here the 2D framework was employed.

The parameters describing desorption kinetics of dissolved organic compounds between solid and solution phases were identical to other studies previously employed in soils or sediments (Chen et al., 2015; Li et al., 2021; Ren et al., 2020). The DIFS model describes the dynamics of dissolved analytes (C_p) and the labile fraction associated with the solid phase (C_l), along with the deployment time to fit first order exchange kinetics (Eq. (3)),



where the rate constants at which the two fractions' magnitudes change are defined as the rate constants of adsorption (k_1) and desorption (k_{-1}), governed by the labile concentration of compounds and the particle concentration of sediment ($P_c = m/V$, where m is the total mass of solid particles and V is the sediment porewater volume) (Eq. (4) and 5).

$$\frac{\partial C_p}{\partial t} = -k_1 \times C_p + (k_{-1} \times P_c \times C_l) \quad (4)$$

$$\frac{\partial C_l}{\partial t} = \frac{k_1 \times C_p}{P_c} - (k_{-1} \times C_l) \quad (5)$$

Rate constants and particle concentrations in the sediment could be used together to fit the linear sorption isotherm, K_{dl} , which defines the partitioning between solution phase and labile solid-phase that could exchange with the solution phase and represents the size of the labile pool in the solid phase. A response time to depletion and associated with desorption processes from solid phase to porewater (K_{dl}) can be equilibrated, T_c , is calculated using Eqs. (6 and 7).

$$K_{dl} = \frac{C_l}{C_p} = \frac{1}{P_c} \times \frac{k_1}{k_{-1}} \quad (6)$$

$$T_c = \frac{1}{k_1 + k_{-1}} \quad (7)$$

When considering C_p was depleted to 0, T_c can reach $1 - (1/e)$, or 63% of the equilibrium solution-solid partitioning value (Honeyman and Santschi, 1988). Labile concentrations (C_l) of antipsychotic drugs were determined by the method of fast-desorbing fraction (Chapter 2.5.2.1) at

the time at which the equilibrium of the first-order three-compartment kinetic model was reached. Concentration of antipsychotic drugs in sediment porewater (C_p) at each deployment time was described in Chapter 2.4. Calculation of the labile phase pool is shown in Section S7.

2.9. Instrumental analysis

Quantifications of nine analytes from all reconstituted samples in methanol was conducted using a Vanquish UHPLC and Q-Exactive™ HF Quadrupole-Orbitrap™ hybrid mass spectrometer (Thermo-Fisher, Mississauga, ON). Analytical details are presented in SM Section S5.

2.10. Data analysis

Statistical analyses were conducted in IBM SPSS Statistics 26. Data obtained from DGT devices and the consecutive extraction method were checked for normality and homogeneity of variance using Levene's test. Since the data did not meet normality criteria and did not show homogeneous variances, non-parametric Kruskal–Wallis tests and Spearman's correlation (significant at $p < 0.05$) were used for comparison and correlation among samples. The desorbing fraction transfer was calculated using MATLAB R2019b.

3. Results and discussions

3.1. DGT performance

The nine target antipsychotic compounds were tested for adsorption to DGT materials, adsorption capability of the binding gel, and the maximum exposure time for DGT sampling. Steady-state sorption concentrations of the nine antipsychotics were quickly reached (< 0.5 h) for DGT molding and diffusive gel. Concentrations remained consistent for 168 h with a negligible fraction ($< 0.01\%$ total mass of the standard solution) adsorbed to DGT moldings (both PTFE and ABS) and diffusive gels. Concentrations of all compounds on the PES filter membrane increased within an hour and reached steady state sorption within 2 h. Proportions of analytes sorbed were negligible ($< 1\%$ of the total mass of the standard solution) for all durations.

Adsorption of the nine analytes to Septra™-ZT binding gel was rapid, within four hours, and became slower as it reached steady-state and the available surface binding sites became saturated (Supplementary Fig. S6). To quantify adsorption capacity of a Septra™-ZT binding gel for the analytes from a given solution, amounts of each analyte adsorbed by Septra™-ZT binding gel vs. the original concentration of each analyte in the solution were plotted (Supplementary Fig. S7). An increasing trend of the adsorbed amount with solute concentration was observed for all nine compounds, ranging from 200 to 2000 $\mu\text{g L}^{-1}$ without a significant

deviation from linearity. At a solute concentration of 5000 $\mu\text{g L}^{-1}$, the amounts adsorbed were not significantly different from that at 2000 $\mu\text{g L}^{-1}$, which indicated that binding sites of the Septra™-ZT adsorbents were saturated.

In order to guarantee the DGT device does not approach equilibrium and to estimate the maximum permissible exposure time for comprehensive sampling, the sorption isotherm of analytes between the measured concentration sorbed by Septra™-ZT (C_{sorbed}) and that in water (C_w) can be described by the distribution constant, which can be calculated by fitting the measured concentrations to the linear sorption model ($C_{\text{sorbed}} = K_{\text{Septra-ZT}} \cdot C_w$). The correlation coefficients in the linear sorption model are good for most compounds (Table 1), whereas the compounds with lesser correlation coefficients (r^2) require more complex sorption models (i.e., Freundlich and Langmuir) to better predict the measured data (Bauerlein et al., 2012). Belles et al. (2017) recommended that it is appropriate to use an adapted linear model to evaluate the sampler's equilibrium. For comprehensive sampling, the DGT devices should be far from the equilibrium at all sampling times and hence the ratio C_{sorbed}/C_w should be less than the $K_{\text{Septra-ZT}}$ values, which can be combined with Eq. (1) and shown as:

$$t_{\text{max-measured}} \ll t_{\text{max-estimated}} = \frac{K_{\text{Septra-ZT}} \delta_{\text{total}}}{D \cdot A} \quad (8)$$

where $t_{\text{max-measured}}$ and $t_{\text{max-estimated}}$ is measured and estimated maximum exposure time to achieve $K_{\text{Septra-ZT}}$ respectively. Our results showed the exposure time for each compound was more than 100 times less than the threshold, which indicates the device remained far from equilibrium conditions at all times.

3.2. Diffusion coefficient

Diffusion coefficients at 25 °C of the nine antipsychotic drugs determined using the diffusion cell method and the slice stacking method are shown (Table 1). D_{cell} and D_{stack} values were not significantly different ($p > 0.05$) for any of the compounds through comparison of triplicate measurements. For the diffusion cell method, the variables from Eq. (S7) were linearly correlated ($r^2 = 0.988\text{--}0.998$) with experimental time (Supplementary Fig. S8). Mean D_{cell} values for the studied antipsychotic drugs ranged from 3.63 to 7.20 $\times 10^{-6}$ $\text{cm}^2 \text{s}^{-1}$, while D_{stack} values ranged from 4.34 to 5.44 $\times 10^{-6}$ $\text{cm}^2 \text{s}^{-1}$. No statistically significant correlations between D and molecular mass of compounds were observed, which might have resulted from the narrow molecular mass range of these compounds (236.27–326.80 Da). This result is consistent with those of previous studies (Urík et al., 2020) for perfluoroalkyl compounds, pharmaceuticals and personal care products with a range of molecular masses of 151 to 377 Da and for

Table 1

Agarose gel diffusion coefficient (D) determined by the diffusion cell method (D_{cell}) and the slice stacking method (D_{stack}) along with associated standard deviation (SD), and estimated diffusion coefficient in water (D_w). Septra™-ZT-water distribution coefficient ($K_{\text{Septra-ZT}}$), with correlation coefficient (R^2) of the linear sorption isotherm in brackets; measured maximum exposure time to achieve equilibrium of the binding gel (t_{max}); and estimated maximum exposure time to achieve $K_{\text{Septra-ZT}}$ for DGT sampler (t'_{max}).

Compounds	D_{cell}	SD	D_{stack}	SD	D_w^a	Log $K_{\text{Septra-ZT}}$	$t_{\text{max-measured}}$	$t'_{\text{max-estimated}}$
	$10^{-6} \text{ m}^2 \text{ s}^{-1}$					L kg^{-1}	h	d
Carbamazepine	5.82	0.79	4.55	0.70	4.46	2.89 (0.83)	1.7	37
Bupropion	4.74	0.69	5.12	0.63	5.19	2.90 (0.74)	4	47
Lamotrigine	5.29	0.65	5.44	0.80	5.41	2.91 (0.92)	1.5	42
Amitriptyline	6.45	0.97	NA	–	4.46	2.89 (0.79)	4	33
Venlafaxine	3.63	0.47	NA	–	4.56	2.89 (0.95)	4	59
Duloxetine	3.80	0.39	NA	–	4.54	2.89 (0.61)	4	57
Fluoxetine	4.68	0.72	4.64	6.20	4.67	2.88 (0.67)	4	44
Citalopram	4.20	0.51	4.34	5.50	4.31	2.89 (0.76)	10	30
Clozapine	5.07	0.65	4.41	4.80	4.39	2.88 (0.84)	4	42

NA: We were unable to measure the D value using the slice stacking method.

^a D values were estimated by the model established by Hayduk and Laudie (1974): $D_w = (13.26 \times 10^{-9}) / (\eta^{1.4} V_m^{0.589})$ where η (cP) is viscosity of water and V ($\text{cm}^3 \text{mol}^{-1}$) is the molar volume of the diffusing analyte at its normal boiling point, which is estimated by the Le Bas increment method (Le Bas, 1915).

polychlorinated biphenyls and polycyclic aromatic hydrocarbons with molecular masses in the range of 128.2 to 429.8 Da) (Rusina et al., 2010). The D_{cell} for carbamazepine ($5.54 \times 10^{-6} \text{ cm}^2 \text{ s}^{-1}$), fluoxetine ($4.72 \times 10^{-6} \text{ cm}^2 \text{ s}^{-1}$), and bupropion ($4.48 \times 10^{-6} \text{ cm}^2 \text{ s}^{-1}$) determined during this study were similar to previously reported values in 1.5% agarose hydrogel, with D values of 5.01×10^{-6} , 4.38×10^{-6} , $5.21 \times 10^{-6} \text{ cm}^2 \text{ s}^{-1}$ for carbamazepine, fluoxetine, and bupropion, respectively (Challis et al., 2016; Fang et al., 2019). The D_{stack} for carbamazepine ($4.55 \times 10^{-6} \text{ cm}^2 \text{ s}^{-1}$) was comparably less than the value ($5.33 \times 10^{-6} \text{ cm}^2 \text{ s}^{-1}$) reported by Urík et al. (2020). Three compounds, e.g., venlafaxine, duloxetine, and amitriptyline ($\text{Log } K_{\text{ow}} = 3.28, 4.68, \text{ and } 4.95$, respectively), failed to measure by the slice stacking method.

Despite different experimental design of two methods, D value derived from the diffusion cell method is simply depended on logarithmic linearization. However, the slice stacking method requires extraction and concentration procedures, causing more uncertainty on the analytical processes. The relative error values in our study for both methods were derived from the model regression fitting to the data. The previous example for estimating the rising uncertainty of D value for copper in DGT sampler was negligible for these factors (e.g., pH and ionic strength) in comparison to the estimated diffusion area and analytical processes. Nevertheless, since slight differences between the two methods, the D values measured using the diffusion cell method was used for calculation DGT-derived concentrations in this study.

3.3. DGT fluxes of antipsychotic drugs in sediment

When concentrations of antipsychotic drugs were averaged by day in water and sediment a declining trend of concentrations in the water column (8–2 cm) and a similar decreasing trend in vertical scale of sediment porewater was observed, except for lamotrigine and bupropion, with the greatest concentrations at a depth of –2 to –4 cm (Fig. 3). This result is consistent with previous observations that increasing dissolved concentrations of organic compounds were found in closer proximity to the sediment (Fernandez et al., 2012; Grimalt et al., 2001). However, for most compounds, except for lamotrigine and bupropion, concentrations in sediment porewater generally remained unchanged ($p > 0.05$) at depths below –2 cm. Concentrations between water and porewater remained within the same order of magnitude for lamotrigine, bupropion, and carbamazepine, while concentrations of other compounds in sediment porewater were approximately 10-fold less than those in the water column. The greatest concentration at 8 cm in water was for carbamazepine ($15.73 \pm 2.14 \mu\text{g L}^{-1}$), which was greater than at 6 cm ($9.58 \pm 1.30 \mu\text{g L}^{-1}$) and 2 cm ($0.54 \pm 0.08 \mu\text{g L}^{-1}$). The greatest mean concentrations among water matrix samples were observed for carbamazepine ($8.61 \mu\text{g L}^{-1}$), followed by duloxetine, amitriptyline, and citalopram ($4.30\text{--}8.16 \mu\text{g L}^{-1}$). Venlafaxine was observed at significantly lesser mean concentrations in both water ($0.077 \mu\text{g L}^{-1}$) and sediment ($0.009 \mu\text{g L}^{-1}$).

Because DGT devices are time-weighted, temporal variability of water concentrations diffusing laterally could not be measured. Therefore, constant concentrations close to the water-sediment interface were assumed for calculating diffusive fluxes. Nevertheless, fluxes were normalized per day, which showed net positive fluxes towards water from sediment (Fig. 3). Overall lesser fluxes ($0.0012\text{--}0.089 \text{ ng cm}^{-2} \text{ d}^{-1}$) were observed for lamotrigine, bupropion, venlafaxine, and duloxetine, while citalopram ($0.10 \text{ ng cm}^{-2} \text{ d}^{-1}$) and fluoxetine ($0.14 \text{ ng cm}^{-2} \text{ d}^{-1}$) had similar fluxes. The greatest flux was found for carbamazepine, indicating that sediment-borne carbamazepine has potential resupply ability to porewater and is prone to partition back to water at the water-sediment interface.

3.4. Three adsorbing fractions of antipsychotic drugs

3.4.1. Fast-desorbing fraction

The plot of S_t/S_0 versus extraction time for desorption of

antipsychotic drugs in sediments sampled at day 1 and day 21 during the DGT deployment period is shown in Fig. 4, where the solid line derived from exponential curve fitting by Eq. (S1) in Section S4. The kinetic parameters obtained from Eq. (S1) are shown in Table S5. Desorption of antipsychotic compounds decreased with increasing the deployment time. Mean desorptions of all compounds in sediment were approximately $21 \pm 2.3\%$ for day 1 and $10 \pm 1.2\%$ for day 21. The F_r values decreased from 0.249 to 0.184 for amitriptyline, 0.403 to 0.331 for bupropion, 0.409 to 0.355 for carbamazepine, 0.261 to 0.127 for citalopram, 0.298 to 0.236 for clozapine, 0.198 to 0.147 for duloxetine, 0.320 to 0.275 for fluoxetine, 0.411 to 0.329 for lamotrigine, and 0.120 to 0.098 for venlafaxine, which indicated that the labile fraction of these compounds decreased in sediments.

Constants k_{rapid} and k_{slow} ranged from 10^{-1} to 10^{-2} h^{-1} and k_{sv} ranged from 10^{-5} to 10^{-6} h^{-1} (Table S6), which is comparable to the magnitude of these parameters from previous labile fraction kinetic studies (Cheng et al., 2019; Trimble et al., 2008; You et al., 2007). The greatest k_{rapid} values both at day 1 and day 21 were found for carbamazepine (0.517 and 0.367 h^{-1}) and lamotrigine (0.531 to 0.383 h^{-1}), while the least values (0.032 and 0.016 h^{-1}) were found for venlafaxine. This result suggests that carbamazepine and lamotrigine could be resupplied from other fractions in sediments while venlafaxine was prone to remain in sediment particles, which might be associated with the ionic interactions of these compounds (e.g., lamotrigine and carbamazepine) (Navon et al., 2011; Zhang et al., 2010) and the potential pool size of compound in sediment. Despite F_r values of all compounds being stable within 24 h extraction period, variations in nonlinear sorption might influence the magnitude (ten Hulscher et al., 1999). The ratios of $F_{24\text{h}}$ to F_r in sediments at day 1 and day 21 showed that the ratio ranged from 77% to 93% (Table S6). This suggests that a single extraction by methanol for 24 h is sufficient to represent the rapidly-desorbing fraction of these drugs. These findings are similar to previous results that equilibrium of F_r could be reached in a short time ($<10 \text{ h}$) during laboratory simulation with a positive linear regression between F_r and $F_{10\text{h}}$ (Cheng et al., 2019).

3.4.2. Stable desorbing fraction

The trend of the concentration in sediments extracted following that of the rapidly-desorbing fraction at each deployment time showed that a slight decreasing concentrations with deployment time were observed for most compounds, whereas duloxetine showed a slightly declining concentration at day 21 (Supplementary Fig. S9 and Table S7). The most significant extent of concentration increase was found for bupropion from 2.21 to $6.32 \mu\text{g kg}^{-1}$ and for fluoxetine from 0.73 to $1.43 \mu\text{g kg}^{-1}$. This result indicates the relative stable state for fraction transfer from stable-desorbing fraction.

3.4.3. Bound residue fraction

Despite the hydrolysis method effectively releasing the bound-residue fraction of organic compounds from sediments (Northcott and Jones, 2000), the uncertainty remains whether the hydrolysis processes or high temperature would influence the analytes and lead to inaccurate quantification. For the accuracy and reliability of analysis results, a single standard solution of each nine antipsychotic drugs was spiked in 10 mL of 1 M NaOH solution at the target concentrations of 10, 100 or $1000 \mu\text{g L}^{-1}$, at $80 \text{ }^\circ\text{C}$ for 24 h to test whether the degradation occurred among nine antipsychotic drugs. Poor recoveries ($< 30\%$) were observed for bupropion and duloxetine while recoveries for other compounds were greater than 80% at all three concentrations. This is consistent with previous observations that bupropion and duloxetine are not resistant to alkaline hydrolysis (Abbas et al., 2012; Rao et al., 2010). Therefore, bupropion and duloxetine are not included in bound-residue fraction discussion. In comparison to concentration of stable-desorbing fraction, except for citalopram, clozapine, and fluoxetine having no significant changes ($p > 0.05$), the concentrations of other compounds showed apparent increases (Table S8). Generally, bound-residue

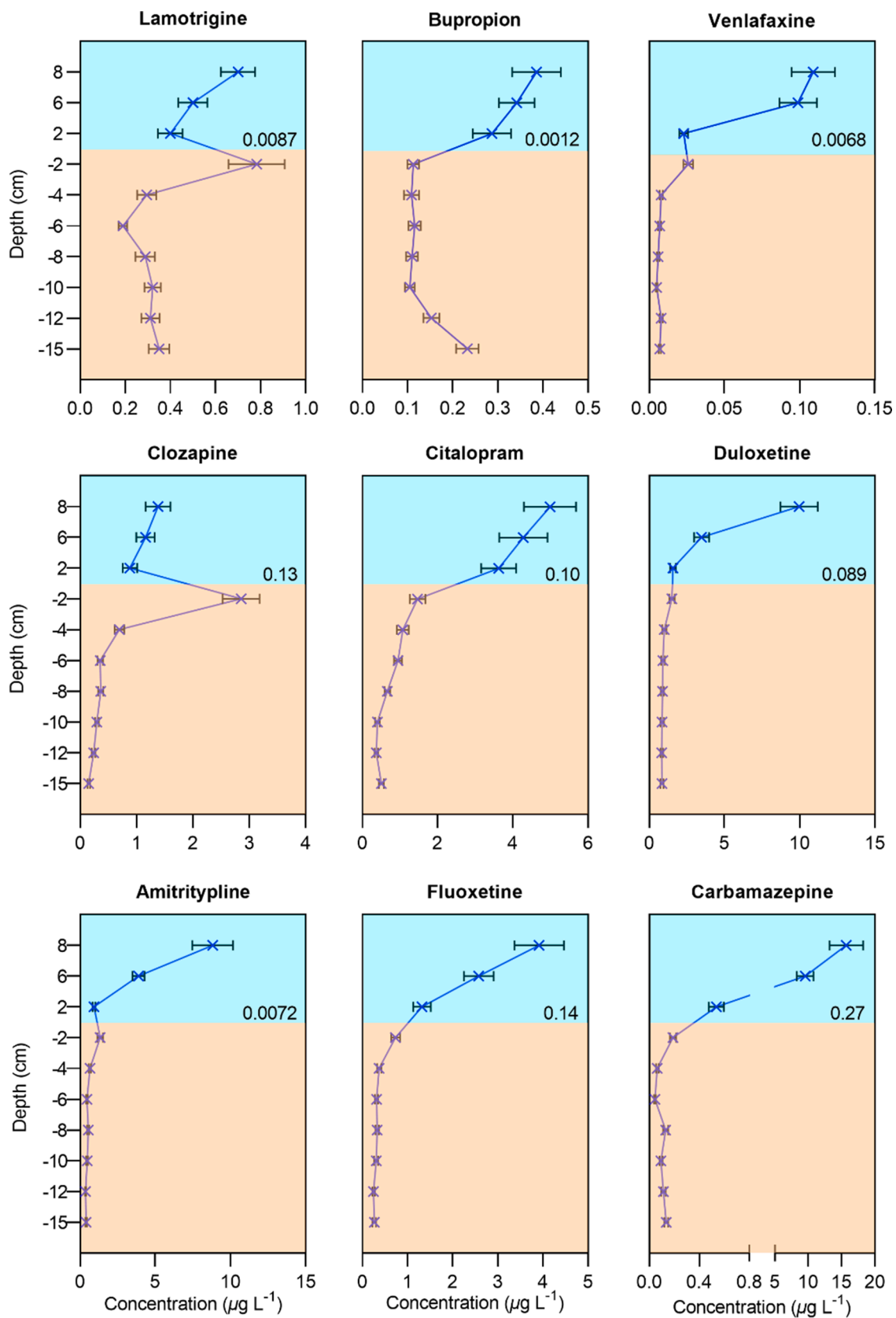


Fig. 3. The plot of profiles of water column and sediment porewater average concentrations of nine antipsychotic drugs measured by DGT devices. The error bars were generated by these data obtained from three DGT devices. The numbers in black were calculated flux ($\text{ng cm}^{-2} \text{day}^{-1}$) from sediment porewater to the water environment. Blue color background represents the water column matrix and light brown color background represents the sediment column matrix. The y-axis is the depth according to DGT field deployment and the x-axis scale is varied based on the better resolution of vertical distribution for each compound.

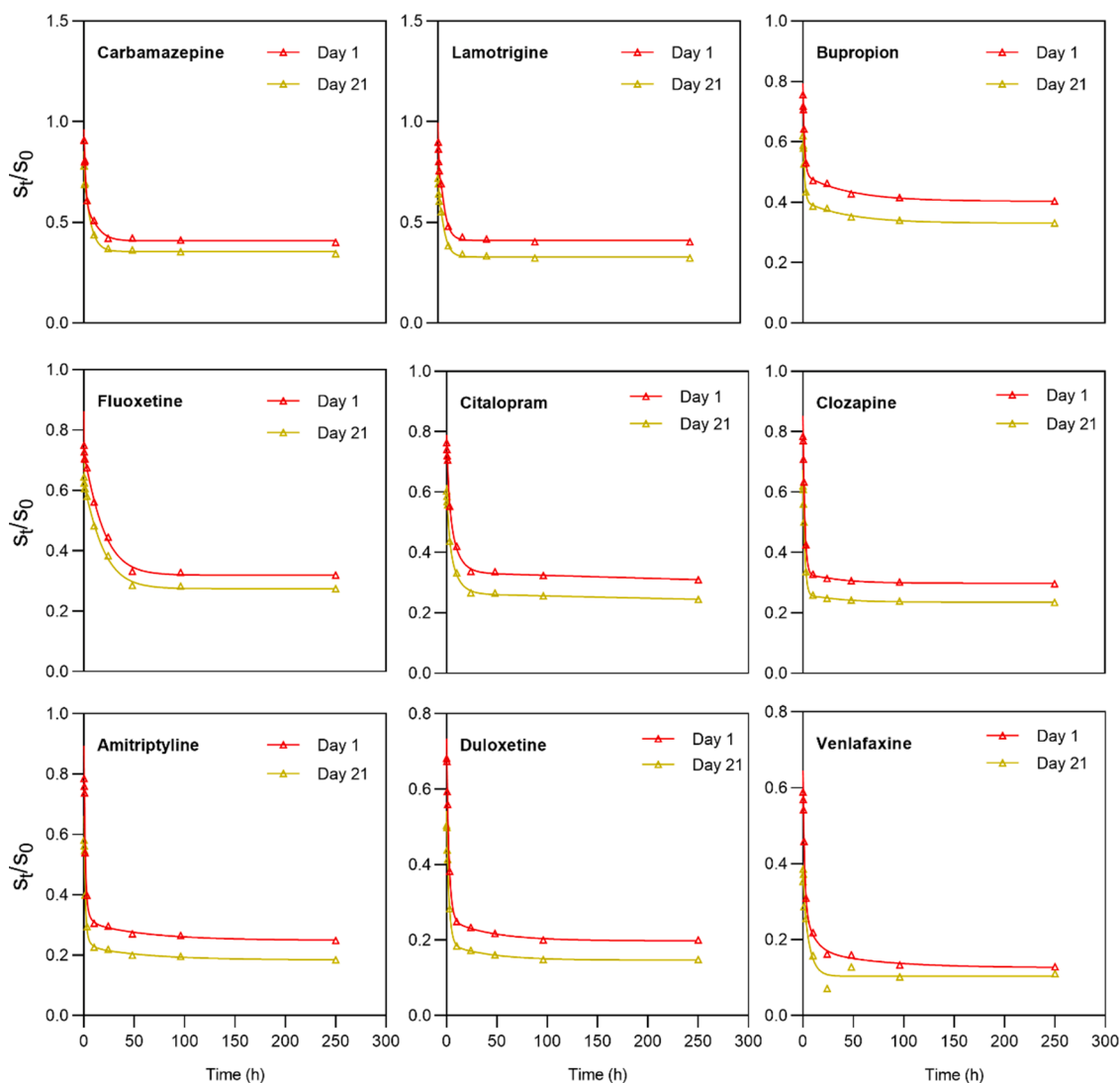


Fig. 4. Desorption kinetics of nine antipsychotic drugs fitted by consecutive methanol extraction. S_t/S_0 was the compound depletion in the sediment at each extraction time (h). Day 1 and Day 21 represent the sediment sampling day in the field during DGT deployment.

concentrations of antipsychotic drugs were increasing with sampling time.

3.5. Transfer of antipsychotic drugs in sediment

During 21 sampling days, the total measured portions of antipsychotic drugs, not considering bupropion and duloxetine, changed from 20% to 70% (Table S9), where total concentration was increased from 1.37 to 4.00 $\mu\text{g kg}^{-1}$ for amitriptyline, 0.46 to 1.28 $\mu\text{g kg}^{-1}$ for carbamazepine, 0.02 to 0.06 $\mu\text{g kg}^{-1}$ for citalopram, 1.60 to 1.99 $\mu\text{g kg}^{-1}$ for fluoxetine, 1.61 to 6.11 $\mu\text{g kg}^{-1}$ for lamotrigine, and 2.13 to 5.51 $\mu\text{g kg}^{-1}$ for venlafaxine, whereas an approximately 50% decrease was observed in clozapine, from 1.83 to 0.94 $\mu\text{g kg}^{-1}$. This suggests a continuous resupply of most selected compounds over time in the real environment while clozapine might experience a poor source pool and different mechanisms of degradation. Microbial degradation has been observed for several antipsychotic drugs (carbamazepine, oxazepam, and codeine) followed a lag period of about 1 day under laboratory simulation (Stein et al. (2008)). Therefore, we could not interpret whether degradation was due to biological processes or photodegradation in real matrices. However, our results demonstrated the certain levels of antipsychotic drugs persist in surface sediments.

The labile, stable-adsorbing and bound-residue fractions of

antipsychotic in sediments is presented in Fig. 5, calculated as the % of the total concentrations of three fractions. This can reflect the resupply ability of compounds to labile fraction. The percentage of labile fraction of antipsychotic drugs all declined with the sampling time, suggesting that the potential bioavailability of these drugs declined. This decline only reflected the static-state distribution of these compounds in sediments. However, while bound-residue or stable-desorbing fraction increased, indicating a risk for fraction transfer to further influence the desorption rate of compounds from sediments to aqueous phase. The relatively slow declines were observed within 6 days, which might be inferred that some competition in sorption sites for different compounds and these compounds might be easier to diffuse to sediment porewater rather than sorption sites. With increasing of sampling time, the gradual decrease of labile fraction could be caused by organic sequestration, clay sorption, and diffusion to sediment micropores. The stable-adsorbing fraction of antipsychotic drugs showed decreases over time for amitriptyline (8% to 5%), carbamazepine (29% to 15%), lamotrigine (27% to 14%), and venlafaxine (46% to 19%); increases for citalopram (43% to 50%), clozapine (17% to 50%), and fluoxetine (48% to 72%). This difference for different compounds might due to the intensity of binding forces or sequestration through the transfer from stable-desorbing fraction to bound-residue fraction.

The bound-residue fraction of antipsychotic drugs from 1 to 21

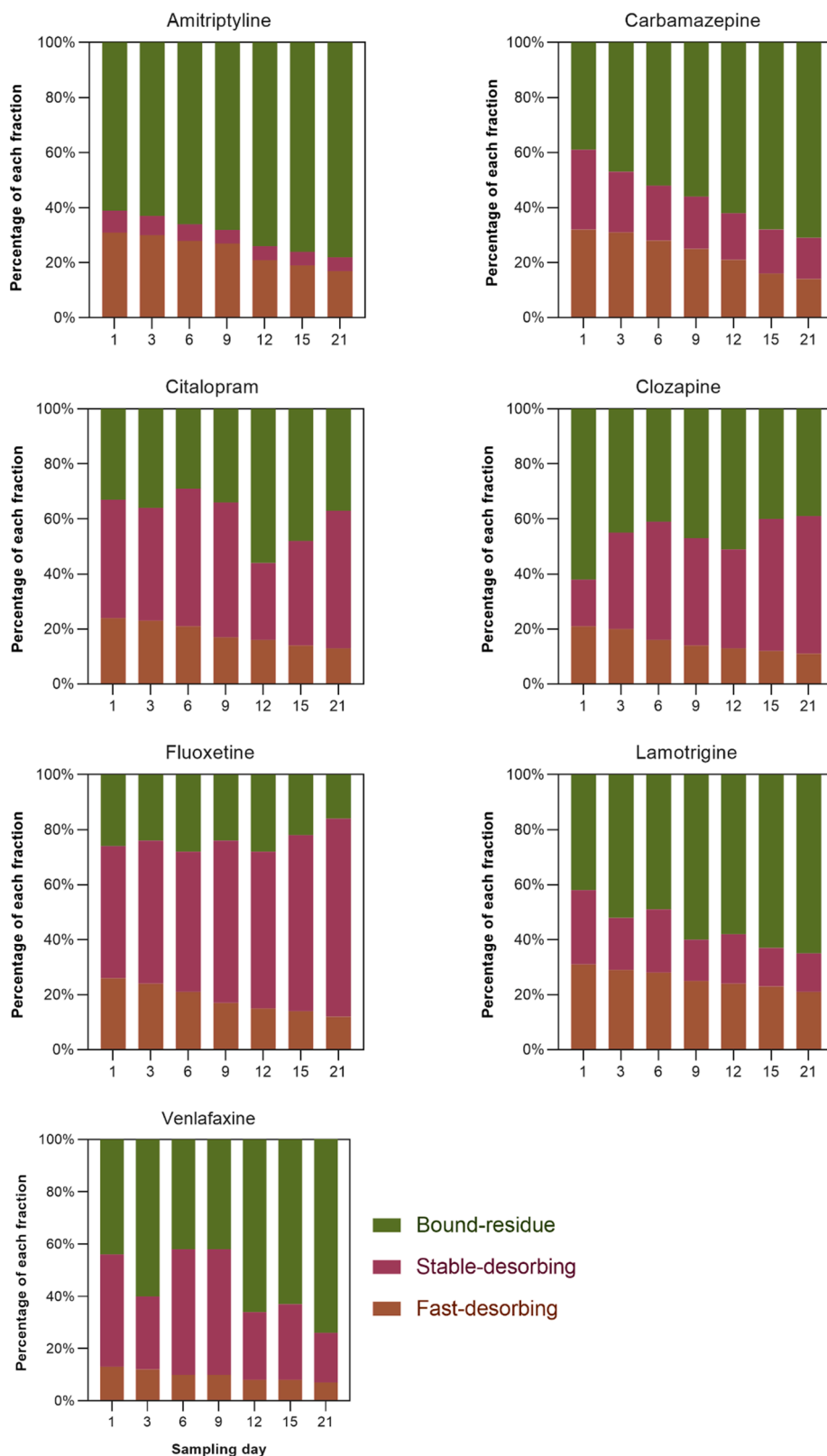


Fig. 5. Rapidly-desorbing (labile), stable desorbing, and bound residue fractions of antipsychotic drugs in sediments from different sampling day during DGT deployment.

d ranged from 61% to 81% for amitriptyline, 39% to 71% for carbamazepine, 33% to 37% for citalopram, 42% to 65% for lamotrigine, 41% to 75% for venlafaxine, 62% to 39% for clozapine, and 26% to 16% for fluoxetine. Despite the bound-residue fraction is generally accompanied

by the other two fractions, increasing bound-residue fraction here for majority of compounds was not directly to the increase of labile fraction, especially for 1 to 6 d This observation is based on the solid sediment capacity of solutes (Cornelissen et al., 1997; Weber and Huang, 1996),

which is, the fraction for some compounds, clozapine and fluoxetine, could not firmly adsorb onto sediment particle surface, and the occurrence of channels and nanopores for sandy texture led to slow diffusion into internal sediment matrix where organic compounds could be

eventually retained. Generally, results reported here indicate that bound-residue fraction of antipsychotic drugs can be an important resupply source for transfer to labile fraction that is continuously increased with sampling days. When a previously developed

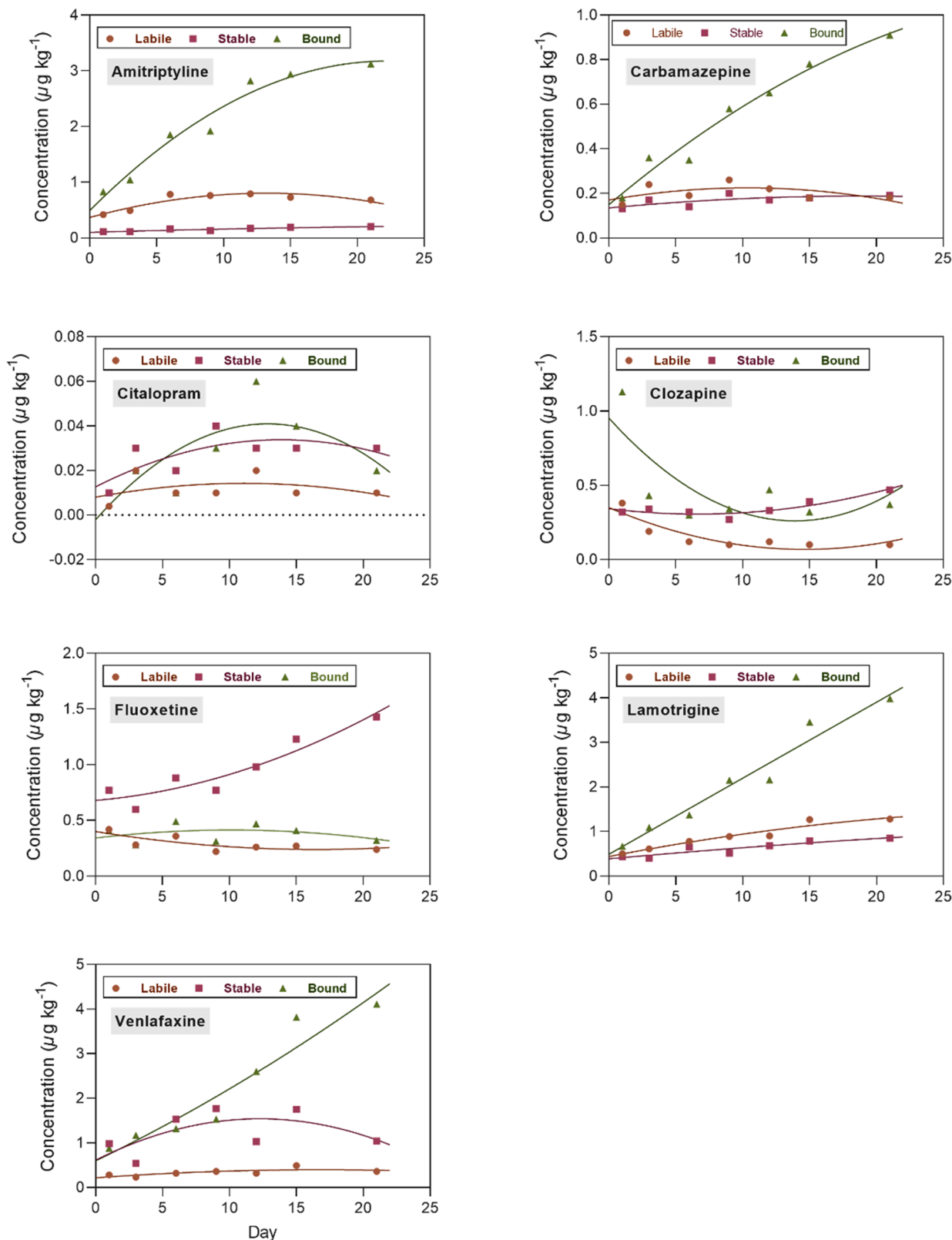


Fig. 6. The experimental data and simulated data for labile, stable-adsorbed, and bound-residue fractions of antipsychotic drugs in sediments during sampling time. The shaped points are experimental results, and lines are model-simulated results (Eq. 15–17).

mathematical model (Cheng et al., 2019) was used to simulate the processes of three fractions' transfer over sampling time without considering degradation conditions (Supplementary Fig. S10) (Eq. (9)–(11)).

$$\frac{dC_{labile}}{dt} = -k_{fs} - k_{fb} + k_{fs}C_{stable} + k_{bf}C_{bound} \quad (9)$$

$$\frac{dC_{stable}}{dt} = -k_{sf} - k_{sb} + k_{fs}C_{labile} + k_{bs}C_{bound} \quad (10)$$

$$\frac{dC_{bound}}{dt} = -k_{bf}C_{bound} - k_{bs}C_{bound} + k_{fb} + k_{sb}C_{stable} \quad (11)$$

where C_{labile} , C_{stable} , and C_{bound} are the concentrations of labile (fast-desorbing), stable-desorbing, and bound-residue fractions, respectively (Table S10). k_{fs} and k_{sf} represent the rate coefficients of partitioning between labile and stable-adsorbing fractions for antipsychotic drugs; k_{fb} and k_{bf} represent the rate coefficients partitioning between labile and bound-residue fractions for antipsychotic drugs; k_{sb} and k_{bs} represent the rate coefficients partitioning between stable-desorbing and bound-residue fractions for antipsychotic drugs. The detailed computation processes of the model are shown in Section S9. The good correlation for model-fitting ($r^2 = 0.915\text{--}0.993$) for three different fractions was observed (Fig. 6). The constant coefficients (k) were not constant during the sampling day and significantly different (Table 2). Overall, k_{fs} is bigger than k_{sf} from the first to last sampling day for all compounds, implying these antipsychotic drugs were prone to retain in the sediment particle rather than sediment porewater. At 21 d, the increasing k_{fs} values suggested that more antipsychotic drugs escaped from labile phase to stable-desorbing fraction. k_{fb} and k_{bf} standing for the ability of sequestering of compounds in sediment particles and its antidromic release, respectively, were nearly 0 at day 1, indicating little labile fraction transferred to bound-residue fraction. This result suggested that antipsychotic drugs had a lag time to be sorbed onto sediments. At 21 d, k_{fb} increased for all drugs except for citalopram, clozapine, and fluoxetine, showing these three drugs had been completely adsorbed by the adsorption sites of sediment particles and pool size for them might be limited as well. The small values of k_{fb} indicated that antipsychotic drugs were partitioned to organic matter and blocked to have a fraction transfer, which is taken as the final fate for organic contaminant (non-bioavailability). Although k_{fb} and k_{bf} were much lower than the other k values, the transfer between bound-residue and stable-desorbing fractions occurred before diffusion into sediment porewater. The increased k_{sb} and k_{bs} for amitriptyline, carbamazepine, lamotrigine, and venlafaxine could represent not irreversible processes, whereas slightly decreased k_{sb} was corresponding to the decreased values of k_{fb} . This could also reflect the dynamic processes in bound-residue fraction where less antipsychotic drugs could be potentially released, to some extent, with accessibility to biota (Cheng et al., 2019; Xing et al., 1996).

3.6. Resupply kinetics and labile size of antipsychotic drugs in sediment

The R value represents the resupply of antipsychotic drugs from the sediment particles to porewater, which responds to the depletion by

Table 2
Rate coefficients (k , d^{-1}) derived by fitting of the transfer model.

	Amitriptyline		Carbamazepine		Citalopram		Clozapine		Fluoxetine		Lamotrigine		Venlafaxine	
	1 d	21 d	1 d	21 d	1 d	21 d	1 d	21 d	1 d	21 d	1 d	21 d	1 d	21 d
k_{fs}	0.0023	0.0043	0.0650	0.0774	0.0032	0.0037	0.0034	0.0039	0.0019	0.0023	0.0022	0.0027	0.0007	0.0008
k_{sf}	0.0040	0.4500	0.0075	0.0087	0.0047	0.0056	0.0052	0.0062	0.0033	0.0038	0.0038	0.0044	0.0013	0.0016
k_{fb}	0.0003	0.0005	0.0009	0.0010	0.0007	0.0050	0.0047	0.0055	0.0002	0.0000	0.0003	0.0003	0.0001	0.0001
k_{bf}	0.0004	0.0004	0.0005	0.0006	0.0019	0.0022	0.0020	0.0024	0.0003	0.0004	0.0004	0.0005	0.0001	0.0001
k_{sb}	0.0065	0.0073	0.0087	0.0101	0.0004	0.0003	0.0003	0.0003	0.0055	0.0012	0.0062	0.0074	0.0018	0.0021
k_{bs}	0.0430	0.0540	0.0120	0.0138	0.0023	0.0027	0.0025	0.0029	0.0353	0.0409	0.0404	0.0465	0.0108	0.0129

The subscript f , s , and b represents fasting-deorbing fraction, stable desorbing fraction, and bound residue fraction, respectively.

DGT devices. The R values in sediment depth of 2–15 cm ranged from 0.15 to 0.41 for carbamazepine, 0.14 to 0.39 for lamotrigine, 0.12 to 0.35 for bupropion, 0.13 to 0.34 for fluoxetine, 0.11 to 0.30 for citalopram, 0.11 to 0.29 for clozapine, 0.09 to 0.25 for amitriptyline, 0.08 to 0.22 for duloxetine, and 0.05 to 0.15 for venlafaxine. When there was no supply from sediment but only diffusion to supply, R_{diff} values derived from DIFS model varied 0.02 to 0.04 for all drugs. Therefore, the sediment for all antipsychotic drugs has ability to supply the positive fluxes from solid phase to sediment solution. In general, R values decreased gradually with deployment time and also with depth (Supplementary Fig. S11), and the differences of that between 8 and 15 cm were not significant ($p > 0.05$) for all drugs, indicating the resupply ability decreased with the depth and resupply could not be quickly provided during the time interval of DGT deployment in real conditions. Additionally, the largest R values were found for carbamazepine and lamotrigine while venlafaxine showed the lowest value, which is similar to the values of k_{sf} and k_{bf} , indicating the low supply to sediment porewater for venlafaxine while carbamazepine and lamotrigine could be resupplied quicker.

The labile antipsychotic drugs in the solid phase could release during DGT deployment to supply those depleted by DGT from sediment solution. The estimated pool size for antipsychotic drugs varied from 0.07 to 0.50 $\mu\text{g kg}^{-1}$ (Table 3) using Eq. (12). The distribution coefficient (K_d), calculated as the ratio of concentration of labile antipsychotic drugs (the equilibrium-reached concentration using consecutive extraction for fast-desorbing fraction at 10 h) to C_p can be used to indicate the labile pool size in sediments. Our K_d values (0.02–32.32 $\text{cm}^3 \text{g}^{-1}$) (Table 3) are within the ranges published (0.01–64 $\text{cm}^3 \text{g}^{-1}$) (Ben-Hur et al., 2003; Li et al., 2021; Ling et al., 2005; Payá-Pérez et al., 1992). The order of average K_d values is followed: carbamazepine > lamotrigine > fluoxetine > bupropion > clozapine > citalopram > amitriptyline > duloxetine > venlafaxine. Interestingly our data showed K_d declined with depth for all drugs except values for fluoxetine were close to 0, and the difference between K_d and K_{dl} was one order of magnitude while no significant decrease with depth was found in K_{dl} . This difference could be due to the solvent extraction to get the maximum compounds from the labile fraction; and the loss for porewater taken over time (e.g., evaporation and redistribution out of field condition). However, it is important that K_d and R values can get the same results for resupply abilities. By calculating labile pool size indicating K_d can be a parameter to use for predicting magnitude of resupply for organic compounds. Considering the alkaline drugs, the slightly decreasing pH and lower organic matter in our sediment had little influence on the adsorption. Additionally, the response time (T_c) and the desorption/adsorption rate constant (k_{-1}/k_1) at different depths (Table 3) showed that the greatest values were found at 2 cm, demonstrating the top layer has the fastest resupply. Ten-fold greater k_{-1} values than k_1 values for all drugs were found, indicating the desorption processes were dominant within 2–15 cm depth.

As the investigated sediment was in a neutral pH environment, the measured antipsychotic drugs remained in their neutral form with adsorption mainly through van der Waals forces or hydrogen bonding, which might be related to the dissolved organic matter for controlling

Table 3

Parameters for analytes at various sediment depths derived from model fits using 2D-DIFS. K_d and K_{dl} (mL g^{-1}) is distribution coefficient derived from methanol extraction and 2D-DIFS, respectively. T_c (s) is the response time. k_{-1} and k_1 (s^{-1}) are the rate constant of desorption and sorption, respectively. $C_{l\text{-estimated}}$ ($\mu\text{g L}^{-1}$) is estimate the labile concentration.

	Depth (cm)	K_d	K_{dl}	T_c	k_{-1}	k_1	$C_{l\text{-estimated}}$
Carbamazepine	1	32.32	0.05	1.72E+05	5.14E-06	6.62E-07	0.07
	4	26.33	0.07	1.97E+05	4.27E-06	8.03E-07	0.09
	8	18.74	0.11	2.20E+05	3.58E-06	9.65E-07	0.12
	15	13.29	0.16	2.46E+05	2.90E-06	1.17E-06	0.20
Lamotrigine	1	21.43	0.05	1.66E+05	5.39E-06	6.32E-07	0.06
	4	17.75	0.07	1.87E+05	4.56E-06	7.89E-07	0.08
	8	12.57	0.10	2.13E+05	3.70E-06	9.86E-07	0.12
	15	9.38	0.15	2.29E+05	3.17E-06	1.20E-06	0.19
Venlafaxine	1	0.04	0.01	1.11E+06	8.87E-07	1.36E-08	0.01
	4	0.03	0.01	1.35E+06	7.24E-07	1.64E-08	0.01
	8	0.03	0.01	1.63E+06	5.94E-07	2.06E-08	0.02
	15	0.02	0.02	1.92E+06	4.95E-07	2.48E-08	0.03
Clozapine	1	7.42	0.12	3.55E+05	2.16E-06	6.53E-07	0.14
	4	6.14	0.18	3.84E+05	1.79E-06	8.14E-07	0.25
	8	4.66	0.25	3.97E+05	1.53E-06	9.87E-07	0.30
	15	3.41	0.37	3.92E+05	1.31E-06	1.24E-06	0.50
Citalopram	1	5.87	0.08	3.28E+05	2.51E-06	5.37E-07	0.12
	4	4.71	0.12	3.68E+05	2.07E-06	6.49E-07	0.15
	8	3.49	0.18	3.88E+05	1.76E-06	8.16E-07	0.22
	15	2.47	0.26	4.05E+05	1.49E-06	9.79E-07	0.32
Fluoxetine	1	12.12	0.15	2.32E+05	3.11E-06	1.20E-06	0.18
	4	10.32	0.05	3.32E+05	2.66E-06	3.53E-07	0.07
	8	7.45	0.07	3.71E+05	2.27E-06	4.27E-07	0.09
	15	5.25	0.11	4.13E+05	1.89E-06	5.32E-07	0.13
Bupropion	1	10.56	0.08	2.39E+05	3.47E-06	7.24E-07	0.10
	4	8.45	0.12	2.64E+05	2.89E-06	8.92E-07	0.15
	8	6.05	0.18	2.86E+05	2.41E-06	1.08E-06	0.21
	15	4.50	0.16	2.10E+05	3.40E-06	1.36E-06	0.20
Duloxetine	1	0.28	0.20	6.08E+05	1.08E-06	5.65E-07	0.25
	4	0.22	0.30	6.19E+05	9.16E-07	7.00E-07	0.39
	8	0.16	0.43	6.16E+05	7.73E-07	8.51E-07	0.50
	15	0.11	0.62	5.92E+05	6.53E-07	1.04E-06	0.75
Amitriptyline	1	0.37	0.08	3.25E+05	2.58E-06	5.01E-07	0.10
	4	0.30	0.12	3.73E+05	2.06E-06	6.21E-07	0.15
	8	0.22	0.17	3.99E+05	1.76E-06	7.54E-07	0.23
	15	0.16	0.26	4.24E+05	1.42E-06	9.34E-07	0.31

the fraction transfer, resupply kinetic characteristics, and labile pool size.

4. Conclusion

This study used *in-situ* deployed DGT devices in water and sediment in field during 21 days. Our results showed positive fluxes of nine antipsychotic drugs from sediment to water. Processes were controlled by the resupply capability from solid phase to sediment porewater. Although rapidly-desorbing (labile) fractions declined during 21 days, the constant coefficients of antipsychotic drugs could be supplied to labile phase quickly from the stable desorbing and bound residue fractions with a lag time. The quickest transfer rate to labile fraction was found for amitriptyline and carbamazepine and the slowest for venlafaxine, which has been also verified by R ratio, response time, and desorption rate constant obtained from DIFS model. The estimated labile pool size from DIFS might not be the best way to reflect the real status, while the labile pool size calculated at equilibrium from a first-order three-compartment kinetic model could fit the changes of R values well. We propose that this could be an auxiliary parameter to understand DIFS output, which is helpful to understand dynamic processes of organic pollutants in sediments.

Funding

Dr. Markus Brinkmann is currently a faculty member of the Global Water Futures (GWF) program, which received funds from the Canada First Research Excellence Funds (CFREF). Mr. Xiaowen Ji was supported through a GWF PhD Excellence Scholarship. Dr. Jonathan Challis was a

Banting Postdoctoral Fellow of the Natural Sciences and Engineering Research Council of Canada (NSERC). This research was supported by a grant from the Western Economic Diversification Canada (Projects # 6578, 6807, and 000012711) towards infrastructure, as well as NSERC Discovery grants to Drs. Markus Brinkmann and John P. Giesy.

Declaration of Competing Interest

The authors declare that they have no known competing financial interests or personal relationships that could have appeared to influence the work reported in this paper.

Data availability statement

Data sets and MATLAB files for this research are available through Ji, Xiaowen (2021), "Data from the DGT devices deployment in the South Saskatchewan River (Clarkboro Ferry)", Mendeley Data, V1, doi: 10.17632/gvtyw95m89.1

Acknowledgement

The authors are grateful to Dr. Xia Liu, Ms. Catherine Estefany Davila Arenas, Ms. Shakya Kurukulasuriya, Ms. Maíra Peixoto Mendes, and Ms. Jocelyn Thresher from the Toxicology center, University of Saskatchewan, for their generous help in the laboratory and the field works. The authors would furthermore like to thank Dr. Jue Ding from Nanjing Hydraulic Research Institute for providing MATLAB packages for calculating desorbing fraction transfer. The authors wish to

acknowledge Prof. Hao Zhang from Lancaster Environment center, Lancaster University for guidance with the 2D-DIFS model. The authors declare no competing financial interests in the publication of this article

Supplementary materials

Supplementary material associated with this article can be found, in the online version, at doi:10.1016/j.watres.2022.118455.

References

- Abbas, S.S., Elghobashy, M.R., Shokry, R.F., Bebawy, L.I., 2012. Stability indicating HPLC and spectrophotometric methods for the determination of bupropion hydrochloride in the presence of its alkaline degradates and related impurity. *Bull. Faculty Pharm.* 50 (1), 49–59. Cairo University.
- Alvarez, D.A., Petty, J.D., Huckins, J.N., Jones-Lepp, T.L., Getting, D.T., Goddard, J.P., Manahan, S.E., 2004. Development of a passive, in situ, integrative sampler for hydrophilic organic contaminants in aquatic environments. *Environ. Toxicol. Chem.* 23 (7), 1640–1648.
- Bäuerlein, P.S., Mansell, J.E., Ter Laak, T.L., de Voogt, P., 2012. Sorption behavior of charged and neutral polar organic compounds on solid phase extraction materials: which functional group governs sorption? *Environ. Sci. Technol.* 46 (2), 954–961.
- Belles, A., Alary, C., Aminot, Y., Readman, J.W., Franke, C., 2017. Calibration and response of an agarose gel based passive sampler to record short pulses of aquatic organic pollutants. *Talanta* 165, 1–9.
- Ben-Hur, M., Letey, J., Farmer, W.J., Williams, C.F., Nelson, S.D., 2003. Soluble and solid organic matter effects on atrazine adsorption in cultivated soils. *Soil Sci. Soc. Am. J.* 67 (4), 1140–1146.
- Benoit, J.M., Shull, D.H., Harvey, R.M., Beal, S.A., 2009. Effect of bioirrigation on sediment–water exchange of methylmercury in Boston Harbor. *Mass. Environ. Sci. Technol.* 43 (10), 3669–3674.
- Bondarenko, S., Gan, J., 2004. Degradation and sorption of selected organophosphate and carbamate insecticides in urban stream sediments. *Environ. Toxicol. Chem.* 23 (8), 1809–1814.
- Challis, J.K., Hanson, M.L., Wong, C.S., 2016. Development and calibration of an organic-diffusive gradients in thin films aquatic passive sampler for a diverse suite of polar organic contaminants. *Anal. Chem.* 88 (21), 10583–10591.
- Chen, C.-E., Chen, W., Ying, G.-G., Jones, K.C., Zhang, H., 2015. In situ measurement of solution concentrations and fluxes of sulfonamides and trimethoprim antibiotics in soils using α -DGT. *Talanta* 132, 902–908.
- Cheng, Y., Ding, J., Xie, X., Ji, X., Zhang, Y., 2019. Validation and application of a 3-step sequential extraction method to investigate the fraction transformation of organic pollutants in aging soils: a case study of dechlorane plus. *Environ. Sci. Technol.* 53 (3), 1325–1333.
- Cornelissen, G., van Noort, P.C.M., Parsons, J.R., Govers, H.A.J., 1997. Temperature dependence of slow adsorption and desorption kinetics of organic compounds in sediments. *Environ. Sci. Technol.* 31 (2), 454–460.
- Soil, A.C.D.-o., Rock, Agency, U.S.E.P., Demars, K.R., Richardson, G.N., Canada, C.E., Yong, R.N., Chaney, R.C., 1995. Dredging, Remediation, and Containment of Contaminated Sediments. ASTM.
- Eek, E., Cornelissen, G., Breedveld, G.D., 2010. Field measurement of diffusional mass transfer of HOCs at the Sediment-water interface. *Environ. Sci. Technol.* 44 (17), 6752–6759.
- Fang, Z., Li, K., Li, Y., Zhang, H., Jones, K.C., Liu, X., Liu, S., Ma, L.Q., Luo, J., 2019. Development and application of the diffusive gradients in thin-films technique for measuring psychiatric pharmaceuticals in natural waters. *Environ. Sci. Technol.* 53 (19), 11223–11231.
- Fernandez, L.A., Lao, W., Maruya, K.A., White, C., Burgess, R.M., 2012. Passive sampling to measure baseline dissolved persistent organic pollutant concentrations in the water column of the palos verdes shelf superfund site. *Environ. Sci. Technol.* 46 (21), 11937–11947.
- Fernandez, L.A., MacFarlane, J.K., Tcaciuc, A.P., Gschwend, P.M., 2009. Measurement of freely dissolved PAH concentrations in sediment beds using passive sampling with low-density polyethylene strips. *Environ. Sci. Technol.* 43 (5), 1430–1436.
- Grimalt, J.O., Fernandez, P., Berdie, L., Vilanova, R.M., Catalan, J., Psenner, R., Hofer, R., Appleby, P.G., Rosseland, B.O., Lien, L., Massabuau, J.C., Battarbee, R.W., 2001. Selective trapping of organochlorine compounds in mountain lakes of temperate areas. *Environ. Sci. Technol.* 35 (13), 2690–2697.
- Harper, M.P., Davison, W., Tych, W., 2000. DIFS—A modelling and simulation tool for DGT induced trace metal remobilisation in sediments and soils. *Environ. Modell. Softw.* 15 (1), 55–66.
- Harper, M.P., Davison, W., Zhang, H., Tych, W., 1998. Kinetics of metal exchange between solids and solutions in sediments and soils interpreted from DGT measured fluxes. *Geochim. Cosmochim. Acta* 62 (16), 2757–2770.
- Hayduk, W., Laudie, H., 1974. Prediction of diffusion coefficients for nonelectrolytes in dilute aqueous solutions. *AIChE J.* 20 (3), 611–615.
- Hayes, M.H., Swift, R., 1978. The chemistry of soil organic colloids. *The Chem. Soil Const.* 179–320.
- He, W., Yang, C., Liu, W., He, Q., Wang, Q., Li, Y., Kong, X., Lan, X., Xu, F., 2016. The partitioning behavior of persistent toxicant organic contaminants in eutrophic sediments: coefficients and effects of fluorescent organic matter and particle size. *Environ. Poll.* 219, 724–734.
- Honeyman, B.D., Santschi, P.H., 1988. Metals in aquatic systems. *Environ. Sci. Technol.* 22 (8), 862–871.
- Iuele, H., Ling, N., Hartland, A., 2021. Characterization of a green expanded DGT methodology for the in-situ detection of emerging endocrine disrupting chemicals in water systems. *Sustain. Chem. Pharm.* 22, 100450.
- Le Bas, G., 1915. *The Molecular Volumes of Liquid Chemical compounds, from the Point of View of Kopp.* Longmans, Green.
- Li, Y., Han, C., Luo, J., Jones, K.C., Zhang, H., 2021. Use of the dynamic technique DGT to determine the labile pool size and kinetic resupply of pesticides in soils and sediments. *Environ. Sci. Technol.*
- Ling, W.T., Wang, H.Z., Xu, J.M., Gao, Y.Z., 2005. Sorption of dissolved organic matter and its effects on the atrazine sorption on soils. *J. Environ. Sci.* 17 (3), 478–482.
- Mechelke, J., Vermeirssen, E.L.M., Hollender, J., 2019. Passive sampling of organic contaminants across the water-sediment interface of an urban stream. *Water Res.* 165, 114966.
- Megahan, W.F., 1999. *Environmental Geology.* Springer, Netherlands, Dordrecht, pp. 552–553.
- Menezes-Blackburn, D., Sun, J., Lehto, N.J., Zhang, H., Stutter, M., Giles, C.D., Darch, T., George, T.S., Shand, C., Lumsdon, D., Blackwell, M., Wearing, C., Cooper, P., Wendler, R., Brown, L., Al-Kasbi, M., Haygarth, P.M., 2019. Simultaneous quantification of soil phosphorus labile pool and desorption kinetics using DGTs and 3D-DIFS. *Environ. Sci. Technol.* 53 (12), 6718–6728.
- Muijs, B., Jonker, M.T.O., 2011. Assessing the bioavailability of complex petroleum hydrocarbon mixtures in sediments. *Environ. Sci. Technol.* 45 (8), 3554–3561.
- Navon, R., Hernandez-Ruiz, S., Chorover, J., Chefetz, B., 2011. Interactions of carbamazepine in soil: effects of dissolved organic matter. *J. Environ. Qual.* 40 (3), 942–948.
- Northcott, G.L., Jones, K.C., 2000. Experimental approaches and analytical techniques for determining organic compound bound residues in soil and sediment. *Environ. Poll.* 108 (1), 19–43.
- Payá-Pérez, A.B., Cortés, A., Sala, M.N., Larsen, B., 1992. Organic matter fractions controlling the sorption of atrazine in sandy soils. *Chemosphere* 25 (6), 887–898.
- Priha, O., Smolander, A., 1999. Nitrogen transformations in soil under Pinus sylvestris, Picea abies and Betula pendula at two forest sites. *Soil Biol. Biochem.* 31 (7), 965–977.
- Rao, D.D., Sait, S.S., Reddy, A.M., Chakole, D., Reddy, Y.R., Mukkanti, K., 2010. Analysis of duloxetine hydrochloride and its related compounds in pharmaceutical dosage forms and in vitro dissolution studies by stability indicating UPLC. *J. Chromatogr. Sci.* 48 (10), 819–824.
- Ren, S., Wang, Y., Cui, Y., Wang, Y., Wang, X., Chen, J., Tan, F., 2020. Desorption kinetics of tetracyclines in soils assessed by diffusive gradients in thin films. *Environ. Poll.* 256, 113394.
- Roberts, T.R., 1984. Non-extractable pesticide residues in soils and plants. *Pure Appl. Chem.* 56 (7), 945–956.
- Rusina, T.P., Smedes, F., Klanova, J., 2010. Diffusion coefficients of polychlorinated biphenyls and polycyclic aromatic hydrocarbons in polydimethylsiloxane and low-density polyethylene polymers. *J. Appl. Polym. Sci.* 116 (3), 1803–1810.
- Schäffer, A., Kästner, M., Trapp, S., 2018. A unified approach for including non-extractable residues (NER) of chemicals and pesticides in the assessment of persistence. *Environ. Sci. Eur.* 30 (1), 51.
- Schwab, K., Brack, W., 2007. Large volume TENAX® extraction of the bioaccessible fraction of sediment-associated organic compounds for a subsequent effect-directed analysis. *J. Soils Sediments* 7 (3), 178–186.
- Semple, K.T., Doick, K.J., Jones, K.C., Burauel, P., Craven, A., Harms, H., 2004. Defining bioavailability and bioaccessibility of contaminated soil and sediment is complicated. *Environ. Sci. Technol.* 38 (12), 228a–231a.
- Skipper, H.D., Wollum II, Arthur G., Turco, R.F., Duane, C.W., 1996. Microbiological aspects of environmental fate studies of pesticides. *Weed Technol.* 10 (1), 174–190.
- Sochaczewski, L., Tych, W., Davison, B., Zhang, H., 2007. 2D DGT induced fluxes in sediments and soils (2D DIFS). *Environ. Modell. Softw.* 22 (1), 14–23.
- Stein, K., Ramil, M., Fink, G., Sander, M., Ternes, T.A., 2008. Analysis and sorption of psychoactive drugs onto sediment. *Environ. Sci. Technol.* 42 (17), 6415–6423.
- Stigliani, W.M., 1991. **Chemical time bombs: definition, concepts, and examples.** ten Hulscher, T.E.M., Vrind, B.A., van den Heuvel, H., van der Velde, L.E., van Noort, P. C.M., Beurskens, J.E.M., Govers, H.A.J., 1999. Triphasic desorption of highly resistant chlorobenzenes, polychlorinated biphenyls, and polycyclic aromatic hydrocarbons in field contaminated sediment. *Environ. Sci. Technol.* 33 (1), 126–132.
- Trimble, T.A., You, J., Lydy, M.J., 2008. Bioavailability of PCBs from field-collected sediments: application of Tenax extraction and matrix-SPME techniques. *Chemosphere* 71 (2), 337–344.
- Urik, J., Paschke, A., Vrana, B., 2020. Diffusion coefficients of polar organic compounds in agarose hydrogel and water and their use for estimating uptake in passive samplers. *Chemosphere* 249, 126183.
- Weber, W.J., Huang, W., 1996. A Distributed Reactivity model for sorption by soils and sediments. 4. Intraparticle heterogeneity and phase-distribution relationships under nonequilibrium conditions. *Environ. Sci. Technol.* 30 (3), 881–888.
- Westrin, B.A., Axelsson, A., Zacchi, G., 1994. Diffusion measurement in gels. *J. Controll. Release* 30 (3), 189–199.
- Xing, B., Pignatello, J.J., Gigliotti, B., 1996. Competitive sorption between atrazine and other organic compounds in soils and model sorbents. *Environ. Sci. Technol.* 30 (8), 2432–2440.
- You, J., Landrum, P.F., Trimble, T.A., Lydy, M.J., 2007. Availability of polychlorinated biphenyls in field-contaminated sediment. *Environ. Toxicol. Chem.* 26 (9), 1940–1948.

Zhang, H., Davison, W., 1995. Performance characteristics of diffusion gradients in thin films for the in situ measurement of trace metals in aqueous solution. *Anal. Chem.* 67 (19), 3391–3400.

Zhang, W., Ding, Y., Boyd, S.A., Teppen, B.J., Li, H., 2010. Sorption and desorption of carbamazepine from water by smectite clays. *Chemosphere* 81 (7), 954–960.

Zhao, Z., Zhang, L., Wu, J., Fan, C., 2009. Distribution and bioaccumulation of organochlorine pesticides in surface sediments and benthic organisms from Taihu Lake, China. *Chemosphere* 77 (9), 1191–1198.

Supplementary Material

A novel passive sampling and sequential extraction approach to investigate desorption kinetics of emerging organic contaminants at the sediment–water interface

Xiaowen Ji^{a,b}, Jonathan K. Challis^c, Jenna Cantin^c, Ana S. Cardenas Perez^a,

Yufeng Gong^c, John P. Giesy^{c, d, e}, Markus Brinkmann^{a, b, c, f*}

^a School of Environment and Sustainability, University of Saskatchewan, Saskatoon, Canada

^b Global Institute for Water Security, University of Saskatchewan, Saskatoon, Canada

^c Toxicology Centre, University of Saskatchewan, Saskatoon, Canada

*^d Department of Veterinary Biomedical Sciences, University of Saskatchewan, Saskatoon,
Canada*

^e Department of Environmental Sciences, Baylor University, Waco, Texas, USA

^f Centre for Hydrology, University of Saskatchewan, Saskatoon, Canada

Contents

Figure S1. The linkage between the mobility of pollutants stored in sediments and climate change.	4
Table S1. Physical-chemical properties of targeted psychoactive drugs.	5
Section S1. Chemical, reagents and standards	6
Figure S2. ABS DGT sediment probe with a PC cap.	7
Figure S3. The site map for DGT deployment and sampling (a), modified from Page 6, Chapter 1–Introduction to the South Saskatchewan River Basin, Water Quality Assessment, South Saskatchewan River Watershed Stewards (https://southsaskriverstewards.ca/projects/water-quality-assessment/), and the field setup picture (b).	8
Table S2. The physicochemical properties of sediment.	9
Section S2. The adsorption tests	10
S2.1 DGT material	10
S2.1 Binding gel	10
Section S3. Procedure of solid-phase extraction (SPE)	12
Section S4. The first-order three-compartment kinetic model for fast-desorbing fraction	13
Figure S4. Schematic diagrams of diffusion cell method (a) and slice stacking method (b).	14
Section S5. Calculation of agarose diffusion coefficient (D)	15
S5.1 The diffusion cell method	15
S5.2 The slice stacking method.	15
S5.3 The D value in different temperatures	16
Section S6. Diffusion between sediment and water	17
Section S7. Estimation of the labile phase pool	18
Section S8. Instrumental analysis	19
Table S3. Precursor (m/z_1) and product ions (m/z_2) with positive ionization mode, collision energy (HCD), and retention time of selected compounds and internal standards (SI) using the a Vanquish UHPLC and full-scan parallel reaction monitoring (PRM) Orbitrap™ mass spectrometer method.	21
Table S4. LOD, LOQ, and MDL ($\mu\text{g L}^{-1}$) for all nine psychotic drugs.	22
Figure S5. Example chromatograms of nine psychotic drugs and their internal standards with scan filter of precursor ion (m/z) for a 500 ng mL ⁻¹ standard solution.	23
Figure S6. Adsorption of nine psychotic drugs on Septra™ ZT binding gel was observed at pH = 7 over 24 hours at a temperature of $21 \pm 0.5^\circ\text{C}$. X-shapes are mean values, and error bars are the standard deviation of measurements from triplicate samplers. The blue curve line is the best fit nonlinear regression line.	24
Figure S7. Steady-state adsorption isotherms of nine psychotic drugs on Septra™ ZT binding gel at pH 7 at 24 hours and a temperature of $21 \pm 0.5^\circ\text{C}$	25
Figure S8. Natural logarithm of ratio of differences between concentration in source and receiving cell at the initial time (ΔC_i) and time t (ΔC) of the diffusion cell method for nine psychotic drugs. Slope of the linear regression is used for calculation of the diffusion coefficient (Eq. 1 and 2 in main text).	26
Table S5. The fractions and rate constants for the rapid, slow, and very slow of nine psychotic drugs	

in sediment at DGT deployment day 1 and 2 predicted by the consecutive methanol extraction. 27

Table S6. The ratio of desorbed fraction of nine psychotic drugs after 10 h methanol extraction the desorbed fraction from all extraction times at sampling time of day 1 and day 21. 28

Figure S9. Logarithm-transformed concentration of nine psychotic drugs in sediment extracted for stable-desorbing fraction after the consecutive extraction for fats-desorbing fraction at each DGT deployment time. The concentration data is shown in Table S8. 29

Table S7. The concentration ($\mu\text{g kg}^{-1}$) of nine psychotic drugs with standard deviation from triplicate samples in sediment extracted for stable-desorbing fraction after the consecutive extraction for fast-desorbing fraction at each DGT deployment time. 30

Table S8. The concentration ($\mu\text{g kg}^{-1}$) of non-degraded psychotic drugs with standard deviation from triplicate samples in hydrolyzed sediment for bound-residue fraction at each DGT deployment time. 30

Table S9. The concentration ($\mu\text{g kg}^{-1}$) of psychotic drugs in the three fractions in sampled sediments at individual time. 31

Figure S10. Illustration of transfer model of antipsychotic drug fractions in sediment. 32

Section S9. The computation processes of fraction transfer modeling. 33

Figure S11. *R* values calculated from different depths in sediments plotted with sampling time. 34

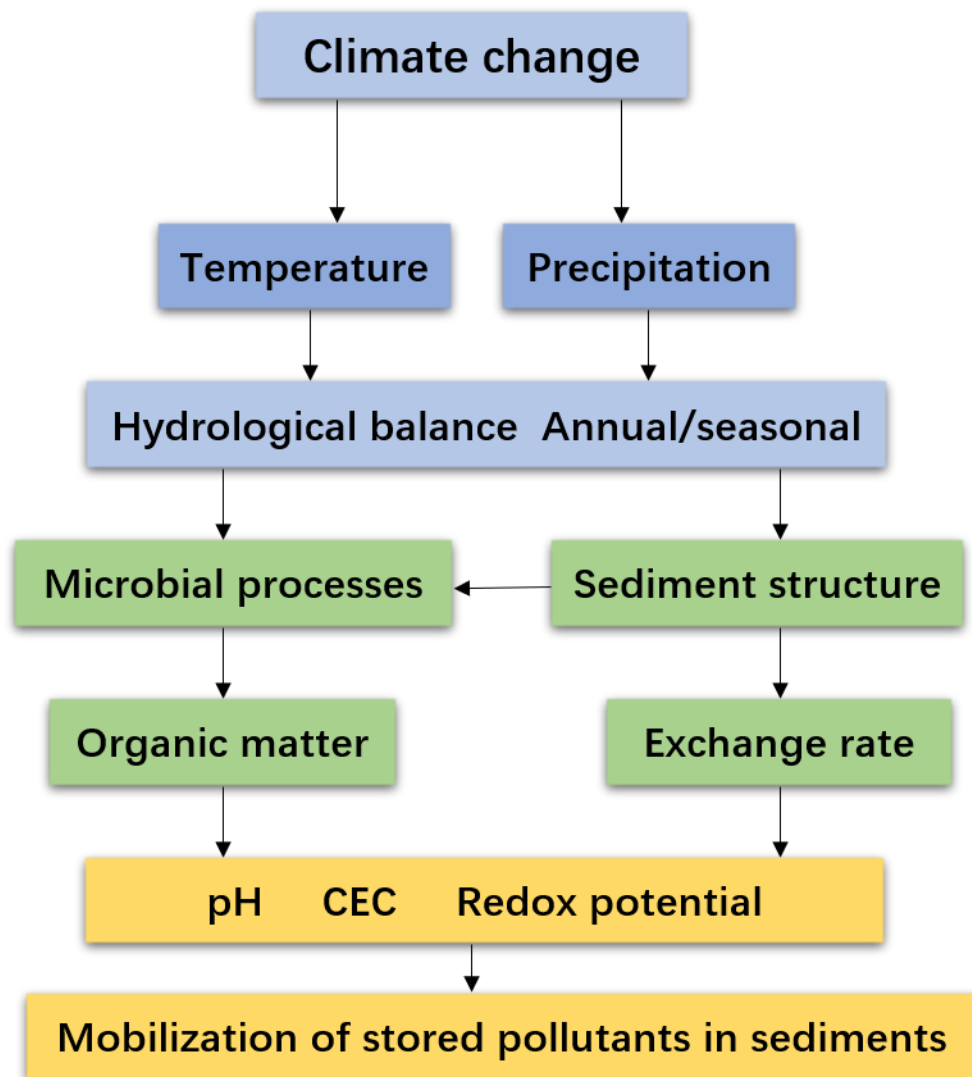
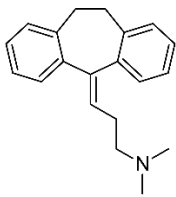
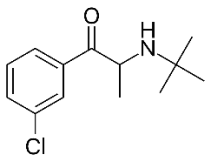
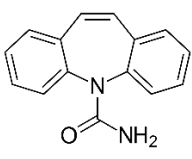
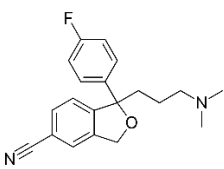
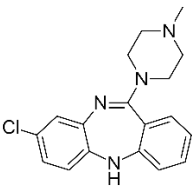
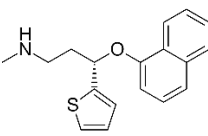
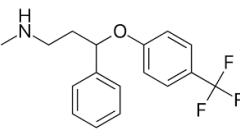
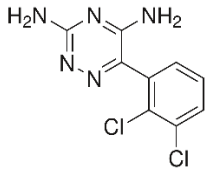
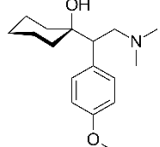


Figure S1. The linkage between the mobility of pollutants stored in sediments and climate change.

Table S1. Physical-chemical properties of targeted psychoactive drugs.

Compound	Structure	CAS	MW	S_w (mg/L)	$pK_{a1,2}$	$\text{Log}K_{ow}$
Amitriptyline		50-48-6	277.4	0.8239	9.4	4.95
Bupropion		34911-55-2	239.74	140.2	8.22	3.85
Carbamazepine		298-46-4	236.27	17.66	13.9	2.25
Citalopram		59729-33-8	324.4	31.09	9.78	3.74
Clozapine		5786-21-0	326.8	11.84	7.5	3.35
Duloxetine		116539-59-4	297.4	10.00	9.7	4.68
Fluoxetine		54910-89-3	309.33	38.35	9.8	4.65
Lamotrigine		84057-84-1	256.09	3127	8.53	0.99
Venlafaxine		93413-69-5	277.4	266.7	10.09	3.28

Water solubilities (S_w) and *n*-octanol-water partitioning coefficients ($\text{Log}K_{ow}$) were predicted using US Environmental Protection Agency's EPISuite™.

Section S1. Chemical, reagents and standards

Amitriptyline, citalopram, duloxetine, lamotrigine, venlafaxine, lamotrigine- ^{13}C ; $^{15}\text{N}_4$], and venlafaxine- d_6 were purchased from Sigma-Aldrich (Oakville, ON). Bupropion, carbamazepine, clozapine, amitriptyline- d_6 , bupropion- d_9 , carbamazepine- d_{10} , citalopram- d_6 , clozapine- d_4 , duloxetine- d_7 , fluoxetine- d_5 were purchased from Toronto Research Chemicals Inc. (North York, ON). Fluoxetine was purchased from Tokyo Chemical Industry Co., Ltd (Tokyo, Japan). A mix stock solution of standards at 1 mg L^{-1} and internal standard mixture at 1 mg L^{-1} were dissolved in pure methanol, which were stored in amber volumetric flasks at a refrigerated cabinet ($-4 \text{ }^\circ\text{C}$). Milli-Q ultrapure water (EMD Milli-Pore Synergy® system, Etobicoke, ON) was used during all experiments and for cleaning purposes. Methanol and dichloromethane were of HPLC grade and purchased from Fisher Scientific (Ottawa, ON).

Optima LC/MS grade formic acid was used as an additive of the LC mobile phase (Fisher Scientific). Agarose, potassium nitrate, and sodium hydroxide from Fisher Scientific were used for making gels, adjusting ionic strength, and hydrolysis of sediments, respectively. All washed glassware was ashed at $500 \text{ }^\circ\text{C}$ for more than 5 h and rinsed by methanol before using.

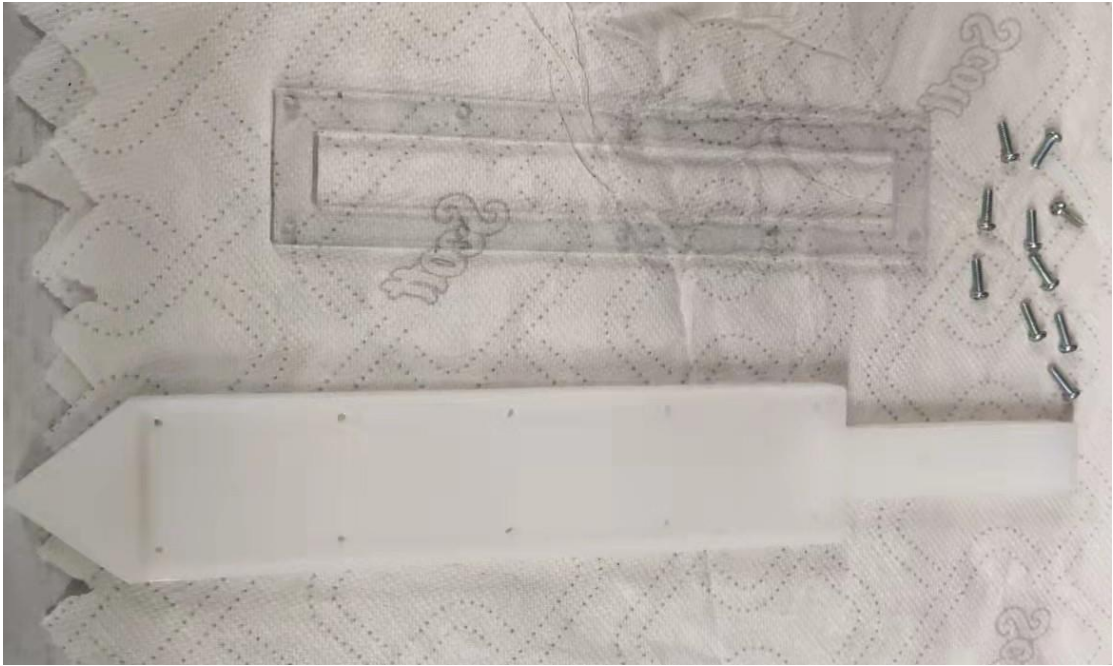


Figure S2. ABS DGT sediment probe with a PC cap.

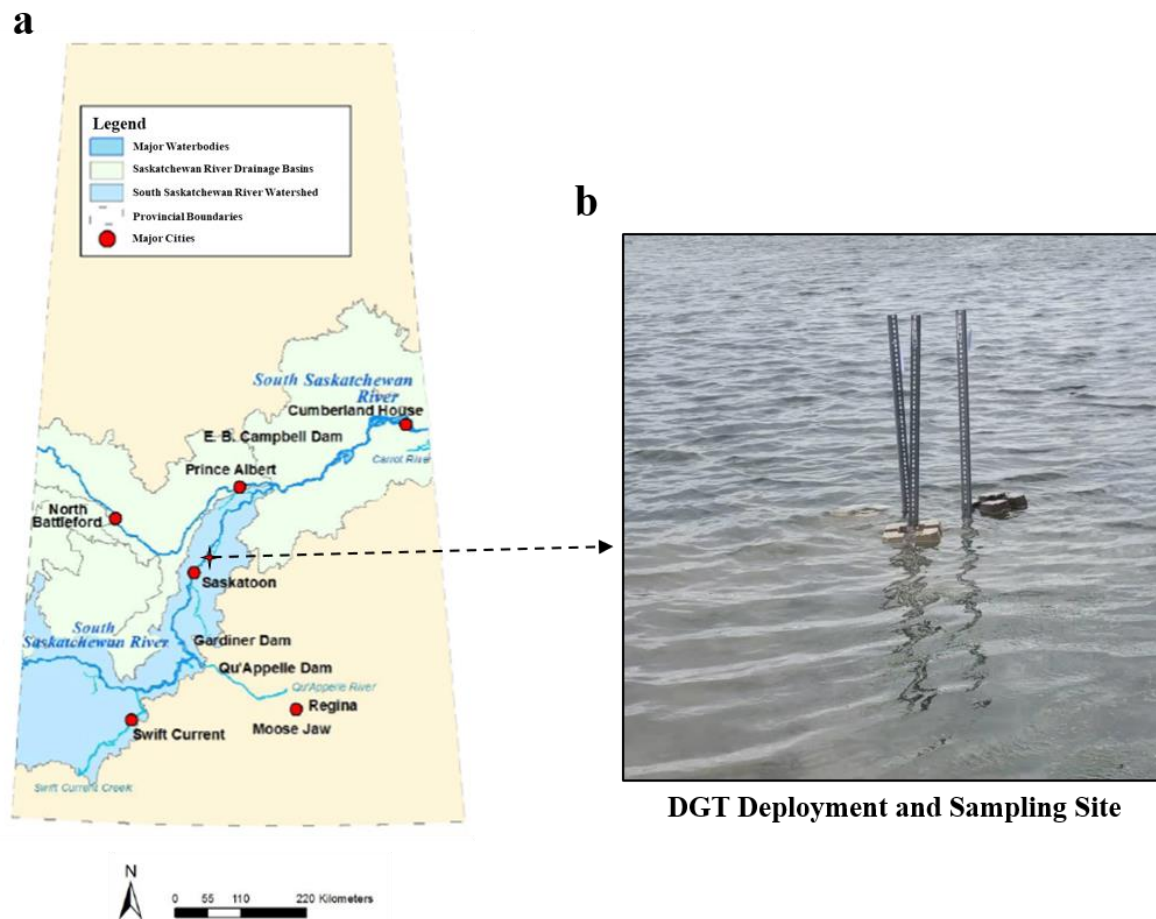


Figure S3. The site map for DGT deployment and sampling (a), modified from Page 6, Chapter 1–Introduction to the South Saskatchewan River Basin, Water Quality Assessment, South Saskatchewan River Watershed Stewards (<https://southsaskriverstewards.ca/projects/water-quality-assessment/>), and the field setup picture (b).

Table S2. The physicochemical properties of sediment.

Depth (cm)	pH	Particle size distribution (%)			Total C (%)	Dissolved organic C (mg L ⁻¹)
		Sand	Silt	Clay		
0-2	7.65	49	36	15	1.4	630
4-6	7.43	48	37	15	1.9	634
6-8	7.12	45	34	21	1.2	658
8-10	6.93	43	32	25	1.5	692
10-12	6.82	42	36	22	1.2	623
12-15	6.97	39	38	23	1.1	631

pH was measured using a ratio of 1:2.5 dry sediment/1 M KCl. Total C was determined by combustion LECO method. Dissolved organic C in soil was extracted by 0.5 M K₂SO₄. Particle size distribution was measured by hydrometer method. All the measurements were conducted in Bureau Veritas Laboratory (Edmonton, AB).

Section S2. The adsorption tests

S2.1 DGT material

For testing of the potential adsorption of analytes in DGT, it is assumed that all DGT materials (molding, diffusive gel, and PES filter membrane) except for the binding gel do not have a significant affinity to adsorb analytes. A standard solution of the nine antipsychotic compounds at $250 \mu\text{g L}^{-1}$ was prepared in 1 mM KNO_3 , and DGT materials were separately exposed to this solution as follows: All DGT materials were separately immersed in 50 mL of the standard solution that was placed in a 100 mL pre-ashed ($550 \text{ }^\circ\text{C}$ in muffle furnace) glass beakers. A magnetic stir bar was added for agitation (4 rpm) at a water temperature of $21 \pm 0.5 \text{ }^\circ\text{C}$. In order to control for potential changes compared to initial concentrations, analytes in solution were quantified at various durations of 0.5, 1, 2, 48, 60, 72, 96 or 168 h. Samples of $190 \mu\text{L}$ were taken from the solution, transferred to LC vials, spiked with $10 \mu\text{L}$ of $1000 \mu\text{g L}^{-1}$ internal standards, and analyzed by LC-MS. DGT moldings, diffusive gels, and PES filter membrane were spiked with 50 ng internal standards, eluted with 5 mL of methanol, and sonicated three times for 10 min. Eluents were evaporated to near dryness by gentle nitrogen gas, reconstituted in 1 mL methanol, then filtered through a $0.2 \mu\text{m}$ polytetrafluoroethylene syringe filter into LC vials before quantification by use of LC-MS.

S2.1 Binding gel

Efficient contact times were determined by placing a binding gel (25 mg SeptraTM ZT sorbent) into a 50 mL glass beaker. Thirty milliliters of the standard solution ($500 \mu\text{g L}^{-1}$) were added to the beaker and magnetically stirred at a constant speed of 4 rpm at $21 \pm 0.5 \text{ }^\circ\text{C}$ for 24 h. Triplicate samples of water were taken at 11 time intervals (0.5, 0.7, 0.8, 1, 1.5, 1.7, 4, 10, 12,

21 or 24 h), spiked with internal standards and then filtered through a 0.2 μm polytetrafluoroethylene syringe filter into LC vials before LC-MS analysis.

Capacities of Septra™ ZT binding gel to adsorb nine (9) antipsychotic compounds were conducted, using the same procedure as the determination for efficient contact time, but at different concentrations (200, 400, 500, 600, 800, 1000, 2000, and 5000 $\mu\text{g L}^{-1}$) at pH of 7 and 21 ± 0.5 °C. Amounts of analytes adsorbed (Q_e) were calculated according to the initial concentrations (C_0) and the steady state concentrations (C_e) as shown in Eq. (S1),

$$Q_e = \frac{(C_0 - C_e)V}{1000m} \quad (\text{S1})$$

where V and m represent the volume of the standard solution (mL) and the mass of adsorbent in the binding gel (mg), respectively.

Section S3. Procedure of solid-phase extraction (SPE)

The sediment porewater or sediment extract was eluted by 250 mL HPLC-grade water (Fisher Scientific, Ottawa, ON) with addition of 50 ng internal standards. Strata-X SPE cartridge (Polymeric Reversed Phase, 30mg/1mL, Phenomenex, CA) was initially preconditioned with 5 mL methanol and 10 mL (methanol: dichloromethane, 50:50), followed with 10 mL HPLC-grade water, after which the cartridge was loaded with the diluted sediment porewater/extracts (pH was adjusted to 7) by a vacuum manifold assisted to suck samples. After the suction of the samples, 5 mL of HPLC-water was added to wash off the remaining traces of samples. Afterwards, the thoroughly-dried cartridge was eluted by 5 mL methanol for two times and followed by the concentration by gentle pure N₂ flow at a temperature of 15 °C. When the eluents were nearly dry, 1 mL methanol was added to reconstitute. Separated triplicate of samples were added of 50 ng internal standards before reconstitution of 1 mL for calculating the recovery rate. The recovery rate was 77% for amitriptyline-d₆, 75% for bupropion-d₉, 104% for carbamazepine-d₁₀, 82% for citalopram-d₆, 86% for clozapine-d₄, 73% for duloxetine-d₇, 74% for fluoxetine-d₅, 92% for lamotrigine-[¹³C;¹⁵N₄], and 75% for venlafaxine-d₆.

Section S4. The first-order three-compartment kinetic model for fast-desorbing fraction

The measure concentrations from the consecutive desorption extraction were fitted with the first-order three-compartment kinetic model, which has been used in soils and sediments (Cornelissen et al., 1997; Pignatello, 1990):

$$\frac{S_t}{S_0} = F_{rap} e^{-k_{rap}t} + F_{slow} e^{-k_{slow}t} + F_{vs} e^{-k_{vs}t} \quad (S1)$$

Where:

$$\frac{dF_{rap}}{dt} = -k_{des}^{rap} F_{rap} \quad (S2)$$

$$\frac{dF_{slow}}{dt} = -k_{des}^{slow} F_{slow} \quad (S3)$$

$$\frac{dF_{vs}}{dt} = -k_{des}^{vs} F_{vs} \quad (S4)$$

Where S_0 and S_t is the mass of psychotic drugs at the beginning ($t=0$) and interval time during the consecutive extraction period. Because this was not a spiking experiment, S_0 was using the total mass of fast-desorbing fraction, stable-desorbing fraction, and bound-residue fraction. S_t/S_0 is the remaining fraction of analytes in the sediment at each time interval. F_{rap} , F_{slow} and F_{vs} are the fractions of rapid desorption, slow desorption, and very slow desorption, respectively. k_{rapid} , k_{slow} , and k_{vs} (h^{-1}) are the first-order rate constants of the rapid desorption, slow desorption, and very slow desorption, respectively.

When the desorption initially occurs in sediments ($t=0$), three compartments can be summed as:

$$F_{rap}^{initial} + F_{slow}^{initial} + F_{vs}^{initial} = 1 \quad (S5)$$

At each time, all compartments reach balance as:

$$F_{rapid} + F_{slow} + F_{vs} + F_{cum} = 1 \quad (S6)$$

Where F_{cum} represents the compartment of cumulative desorption.

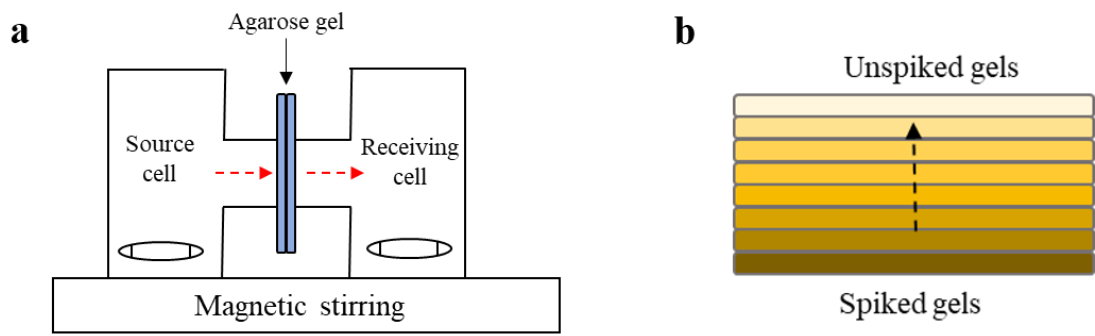


Figure S4. Schematic diagrams of diffusion cell method (a) and slice stacking method (b).

Section S5. Calculation of agarose diffusion coefficient (D)

S5.1 The diffusion cell method

A value for D_{cell} can be calculated by eq. (1) (Cussler, 2009) when the hydrogel-water distribution coefficient = 1 due to negligible adsorption to the agarose gel (Section S2).

$$D_{\text{cell}} = \frac{1}{\beta t} \ln\left(\frac{C_S^i - C_R^i}{C_S(t)C_R(t)}\right) \quad (\text{S7})$$

in which,

$$\beta = \frac{A}{\delta} \left(\frac{1}{V_S} - \frac{1}{V_R} \right) \quad (\text{S8})$$

C^i and $C(t)$ represent the initial concentration of the analyte and the concentration at time (t) respectively. The subscripts S and R represent source and receiving cell, respectively. A is the superficial area of the agarose gel, δ is the thickness of the agarose gel, and V is the volume of solution in each cell. The term $\ln\left(\frac{C_S^i - C_R^i}{C_S(t)C_R(t)}\right)$ in eq. (S7) was plotted against experimental time, which was fitted using linear regression. Then, the value of D_{cell} was obtained from the slope of the regression.

S5.2 The slice stacking method

The D_{stack} value was calculated for each individual exposure time by fitting data to the model in Eq. (S9) derived from Crank (1979).

$$C = C_i \left(\frac{h}{l} + \frac{2}{\pi} \sum_{n=1}^{\infty} \frac{1}{n} \sin\left(\frac{n\pi h}{l}\right) \exp\left(-\frac{D_{\text{stack}} n^2 \pi^2 t}{l^2}\right) \cos\left(\frac{n\pi x}{l}\right) \right) \quad (\text{S9})$$

where C and C_i (ng g^{-1}) represent the analyte concentration at the distance of the top of the stack (cm) and the measured initial concentration of the spiked gels, respectively. h and l (cm) represent the thickness of the stack and the thickness of the spiked gels respectively. t (s) is the exposure time

and n is the summation index. The measured D_{stack} values was averaged across all exposure times experiments, in which the ultimate concentrations of spiked gels range from 40 to 75% of initial concentrations in consideration of an obvious concentration gradient. For minimum of the uncertainty, the data out of this range was abandoned.

S5.3 The D value in different temperatures

For D calculation for different temperatures, they were calculated from D values for 25 °C (D_{25}) using an empirical formula established by Yuan-Hui and Gregory (1974) (Eq. S10):

$$\log \frac{D_{25}(273+T)}{298} = \log D_T - \frac{1.37023(T-25) + 0.000836(T-25)^2}{109+T} \quad (\text{S10})$$

Section S6. Diffusion between sediment and water

The flux of dissolved antipsychotic drugs by diffusion between sediment and water (F_{sw} , ng m⁻² d⁻¹) can be calculated using Eq. (S11).

$$F_{sw} = -k_{sw} \left(C_{DGT-w} - \frac{C_{DGT-s}}{K_s} \right) \quad (S11)$$

where C_{DGT-s} is the concentration of analytes in sediments measured using the DGT probe (ng kg⁻¹), and K_s is the sediment-water partitioning coefficient (cm³ kg⁻¹) based on Schwarzenbach et al. (2017) using $f_{oc}=0.014$ in the studied sediment, and k_{sw} is the diffusion coefficient (cm d⁻¹) between water and sediment, which can be calculated using Eq. (S12). The term C_{DGT-s}/K_s indicates the dissolved concentration in sediment porewater.

$$k_{sw} = \frac{D_w}{\delta_{bl}} \quad (S12)$$

where δ_{bl} is the thickness of boundary layer (m). In this study, the small scale of turbulent flows was considered only for vertical transport induced by cascading turbulent eddies due to the limited transverse transport distance. The vertical turbulent eddies are defined as the distance from the sediment surface where overturning turbulent motion is governed by molecular viscosity. In this study, δ_{bl} could not be directly characterized using the linear concentration gradient where the transport is dominant by molecular diffusion. δ_{bl} of 0.2 mm was used for all analytes through the calculation based on a kinematic viscosity of 0.013 cm² s⁻¹ and a fraction velocity of 0.5 cm s⁻¹ (Sherwood et al., 2002; Wang et al., 2001).

Section S7. Estimation of the labile phase pool

In this study, $C_{DGT, i=21d}$ derived from the last day of DGT deployment (21 d) was used to calculate the effective concentration by Eq. (11) to define the available antipsychotic drugs in sediment porewater and the labile pool from the solid phase (Zhang et al., 2006). The effective concentration ($C_{e, i=21d}$) expresses the concentration ranges of C_{DGT} in the sediment pools for antipsychotic drugs, which describes the desorption behavior of antipsychotic drugs from the solid phase during the DGT deployment (Eq. S13).

$$C_{e,i} = \frac{C_{DGT, i=21d}}{R_{diff, i=21d}} \quad (S13)$$

where R_{diff} is the ratio of C_{DGT} to C_p in the hypothetical case that the depleted antipsychotic drugs are only supplied from diffusion in porewater without supplies from the solid phase. R_{diff} was calculated by the 2D-DIFS model, which requires sediment porosity (ϕ), particle concentration (P_c), and diffusion layer thickness (δ_{total}) according to the simulation parameter requirements (Harper et al., 1998).

The best fitted K_{dl} was used to estimate the labile concentration ($C_{l-estimated}$) of antipsychotic drugs, expressed as Eq. (S14).

$$C_{l-estimated} = C_p \times K_{dl} \quad (S14)$$

The $C_{l-estimated}$ was compared to the concentrations at the beginning and interval time during the consecutive extraction period.

Section S8. Instrumental analysis

LC separation was achieved with a Kinetex 1.7 μm XB-C₁₈ LC column (100 \times 2.1 mm) (Phenomenex, Torrance, CA) by gradient elution with 95% water + 5% methanol (A) and 100% methanol (B), both containing 0.1% formic acid (Optima MS grade) at a flow rate of 0.2 mL min⁻¹ and a column temperature of 40 °C. The gradient method started at 10% B, ramping linearly to 100% B over 7 min, was held for 1.5 min, and returned to starting conditions for column re-equilibration between 8.5 – 11 min.

Samples were ionized using positive mode heated electrospray ionization (HESI). The Q-Exactive Orbitrap method used the following source parameters: sheath gas flow = 35; aux gas flow = 10; sweep gas flow = 1; aux gas heater = 400 °C; spray voltage = 3.8 kV; S-lens RF = 60; capillary temperature = 350 °C. A Full MS/parallel reaction monitoring (PRM) method was used with the following scan settings: 120,000/15,000 resolution, AGC target = $1 \times 10^6/2 \times 10^5$, max injection time = 50 ms/50 ms, full MS scan range of 80-500 m/z and PRM isolation window of 2.0 m/z and multiplexing count of 4.

Batch analyses of samples were conducted by running calibration standards at the beginning and end of each sample batch along with blanks run between replicate treatment sets and 50 $\mu\text{g L}^{-1}$ single calibration standards after running calibration standards and every 20 samples as a QA/QC protocol. A nine-point calibration curve ranging from 0.01 – 950 $\mu\text{g L}^{-1}$ and spiked with 50 $\mu\text{g/L}$ IS was used for quantification by isotope dilution (linearity > 0.99 for all analytes). All data acquisition and processing were conducted using Xcalibur v. 4.2 (Qual and Quan browser). The quantification of each analyte was according to precursor and product ions, and retention time (**Table S3** and **Figure S5**). The method detection limits (MDL), limits of quantitation

(LOQ), and limits of detection (LOD) are reported (**Table S4**). When the concentrations of analytes were below the detection limit, the substitution method ($\text{LOD}/\text{square root of } 2$) was used (Ganser and Hewett, 2010). MDL were calculated using the average blank DGT (three extra DGT devices were taken to the field) concentration in each DGT retrieval time plus three times the standard deviation (3σ). The extraction and processing procedures of DGT field blanks were the same as described in the main text. The instrumental LOD and LOQ were regarded as the low concentration of analyte with a measured signal/noise (S/N) of 3 and 10, respectively ($\text{LOD} = 3\sigma_{\text{blank}}/\text{slope}$, $\text{LOQ} = 10\sigma_{\text{blank}}/\text{slope}$). Slopes were obtained from 9-points calibration curve.

Table S3. Precursor (m/z1) and product ions (m/z2) with positive ionization mode, collision energy (HCD), and retention time of selected compounds and internal standards (SI) using the a Vanquish UHPLC and full-scan parallel reaction monitoring (PRM) Orbitrap™ mass spectrometer method.

Compound	m/z1	m/z2	HCD	Retention time (min)*
Amitriptyline	278.190	233.132	35	7.57–7.76
SI Amitriptyline-D ₆	284.228	233.132	35	7.57–7.74
Bupropion	240.115	184.052	25	5.45–5.64
SI Bupropion-D ₉	249.171	185.059	25	5.43–5.60
Carbamazepine	237.102	194.097	35	8.08–8.09
SI Carbamazepine-D ₁₀	247.165	204.159	35	8.04–8.05
Citalopram	325.171	109.045	40	6.59–6.77
SI Citalopram-D ₆	331.209	109.045	40	6.59–6.78
Clozapine	327.137	270.079	35	6.31–6.48
SI Clozapine-D ₄	331.162	272.092	35	6.29–6.46
Duloxetine	298.126	183.081	30	7.53–7.69
SI Duloxetine-D ₇	305.170	189.118	30	7.50–7.71
Fluoxetine	310.141	148.112	25	7.70–7.89
SI Fluoxetine-D ₅	315.173	153.144	25	7.70–7.88
Lamotrigine	256.015	210.983	70	4.67–4.76
SI Lamotrigine-[¹³ C; ¹⁵ N ₄]	261.007	213.980	70	4.67–4.75
Venlafaxine	278.211	260.201	25	6.20–6.29
SI Venlafaxine-D ₆	284.249	266.239	25	6.14–6.29

* The retention time was shifted for each sequence run due to the pressure changes of LC column. The difference of retention time changes was within 3%.

Table S4. LOD, LOQ, and MDL ($\mu\text{g L}^{-1}$) for all nine psychotic drugs.

Compound	LOD	LOQ	MDL
Venlafaxine	0.22	0.73	0.03
Fluoxetine	1.38	2.58	0.02
Clozapine	0.35	1.19	0.03
Citalopram	2.05	2.45	0.01
Duloxetine	0.19	0.63	0.11
Amitriptyline	1.71	5.70	0.06
Bupropion	0.33	1.11	0.03
Carbamazepine	1.16	3.97	0.01
Lamotrigine	0.18	0.63	0.02

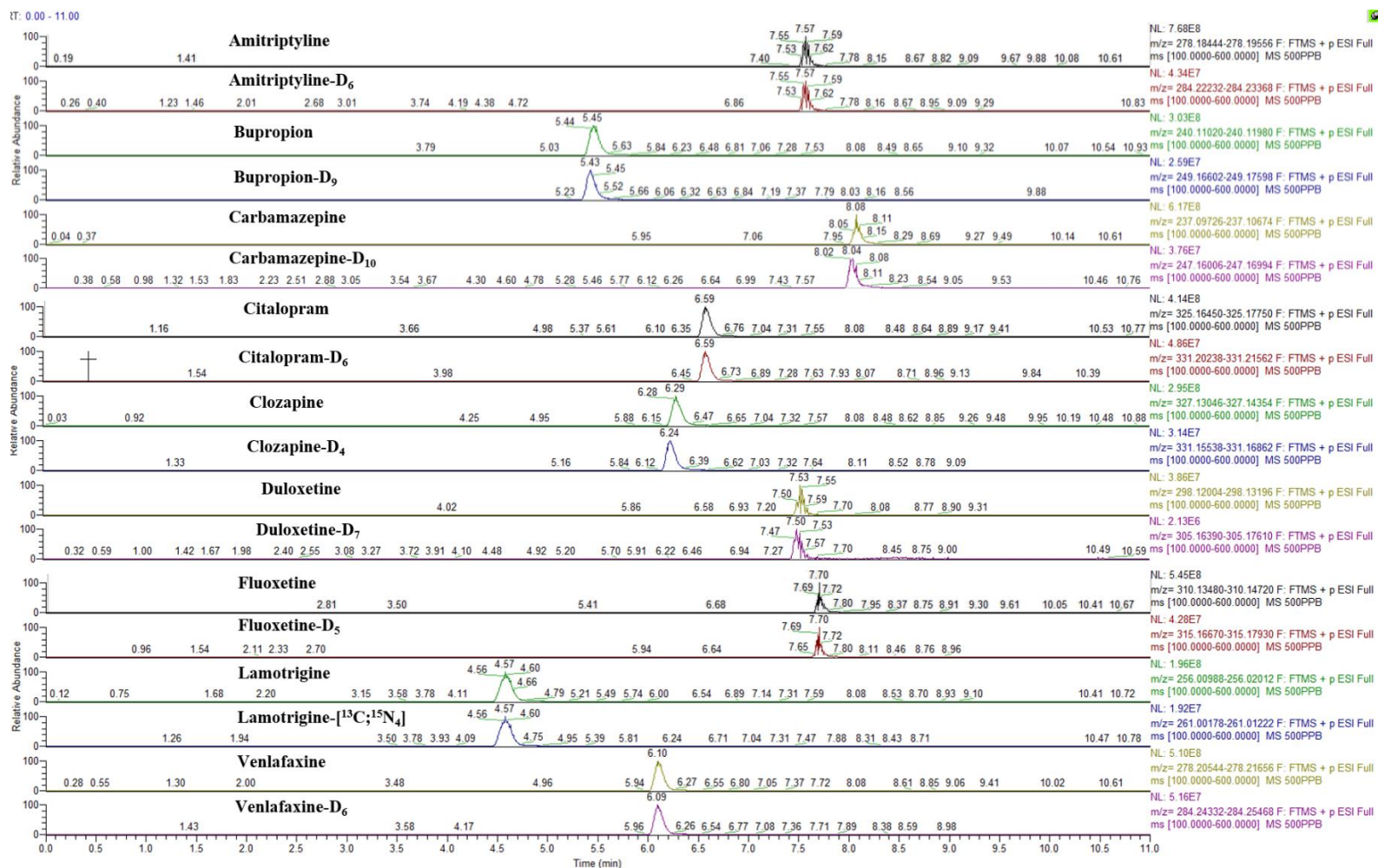


Figure S5. Example chromatograms of nine psychotic drugs and their internal standards with scan filter of precursor ion (m/z) for a 500 ng mL⁻¹ standard solution.

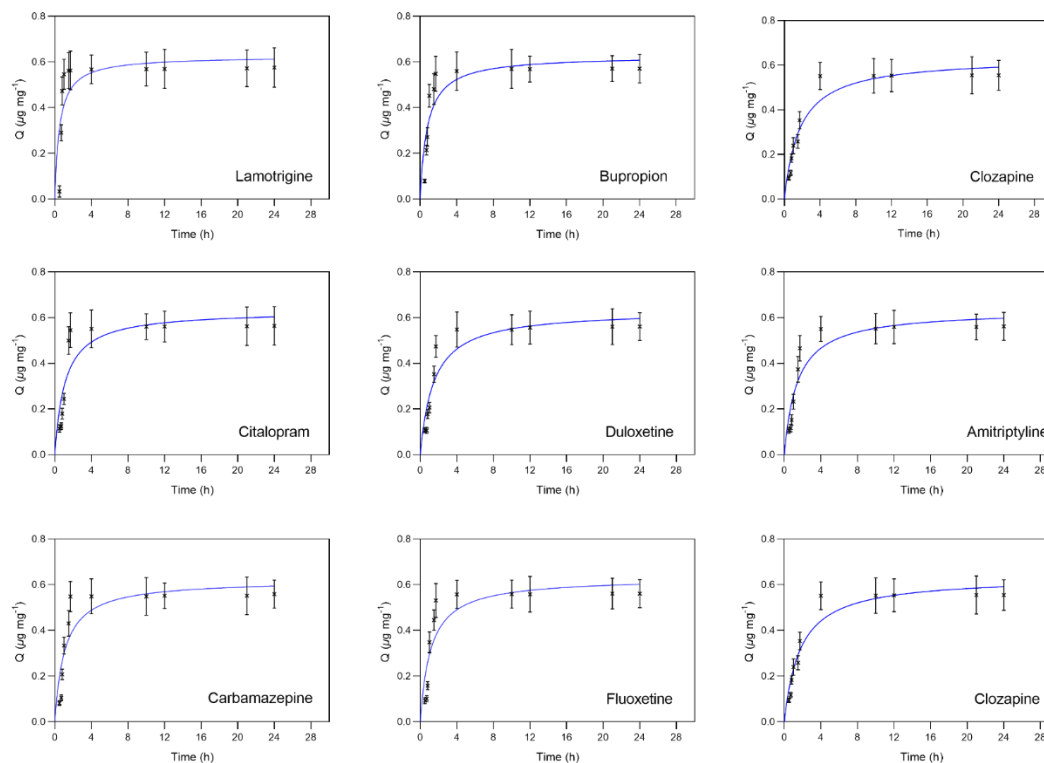


Figure S6. Adsorption of nine psychotic drugs on Sepra™ ZT binding gel was observed at pH = 7 over 24 hours at a temperature of $21 \pm 0.5^\circ\text{C}$. X-shapes are mean values, and error bars are the standard deviation of measurements from triplicate samplers. The blue curve line is the best fit nonlinear regression line.

The adsorption amount ($Q, \mu\text{g mg}^{-1}$) was calculated from $Q = \frac{(C_0 - C_i) \times V}{1000m}$, in which C_0 and C_i represent the initial concentration and concentration from each sampling time, respectively, and V and m represent the volume of the standard solution (mL) and the mass of adsorbents in the binding gel (mg), respectively.

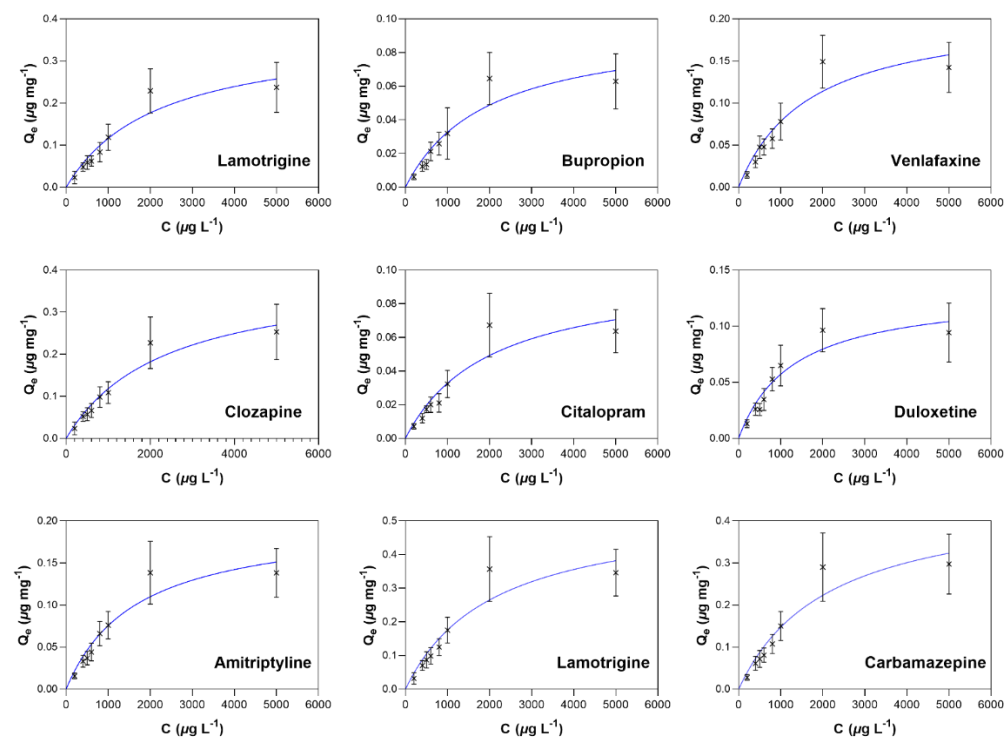


Figure S7. Steady-state adsorption isotherms of nine psychotic drugs on Sepra™ ZT binding gel at pH 7 at 24 hours and a temperature of $21 \pm 0.5^\circ\text{C}$. X-shape are mean values, error bars are the standard deviation of measurements from triplicate samplers. The blue curve line is the best fit nonlinear regression line. C ($\mu\text{g L}^{-1}$) represents different concentrations of analyte standard solution. The steady-state adsorption amount (Q_e , $\mu\text{g mg}^{-1}$) was calculated from $Q_e = \frac{(C_0 - C_e) \times V}{1000m}$. C_0 and C_e represent the initial concentration and the reached steady-state concentration, respectively. V and m represent the volume of the standard solution (mL) and the mass of adsorbents in the binding gel (mg), respectively.

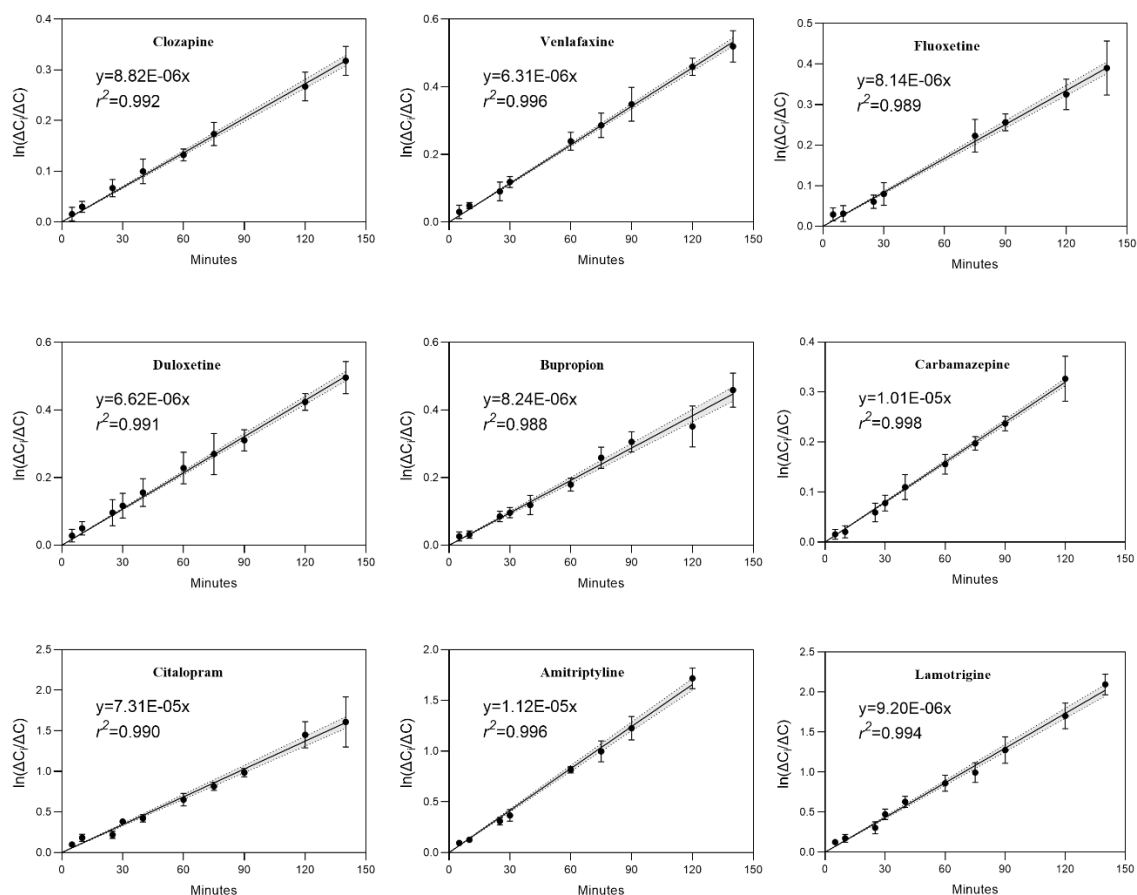


Figure S8. Natural logarithm of ratio of differences between concentration in source and receiving cell at the initial time (ΔC_i) and time t (ΔC) of the diffusion cell method for nine psychotic drugs. Slope of the linear regression is used for calculation of the diffusion coefficient (Eq. 1 and 2 in main text). The error bar represents the triplicate data used to calculate the ratio from the experiments. The grey area composed by dotted line represents the ratio ranged in 95% confidence interval.

Table S5. The fractions and rate constants for the rapid, slow, and very slow of nine psychotic drugs in sediment at DGT deployment day 1 and 2 predicted by the consecutive methanol extraction.

Compound	Day	F_{rapid}	k_{rapid}	F_{slow}	k_{slow}	F_{vs}	k_{vs}	r^2
Amitriptyline	1	0.249	0.174	0.322	0.021	0.417	0.000002	0.985
	21	0.184	0.083	0.303	0.015	0.500	0.000001	0.988
Bupropion*	1	0.403	0.466	0.429	0.145	0.155	0.000013	0.998
	21	0.331	0.415	0.343	0.103	0.314	0.000009	0.998
Carbamazepine	1	0.409	0.517	0.516	0.342	0.063	0.000031	0.991
	21	0.355	0.367	0.323	0.316	0.310	0.000029	0.992
Citalopram	1	0.261	0.143	0.378	0.121	0.349	0.000011	0.998
	21	0.127	0.042	0.353	0.025	0.508	0.000002	0.998
Clozapine	1	0.298	0.152	0.387	0.013	0.303	0.000001	0.998
	21	0.236	0.120	0.343	0.014	0.410	0.000001	0.995
Duloxetine*	1	0.198	0.150	0.350	0.024	0.440	0.000002	0.997
	21	0.147	0.113	0.311	0.018	0.531	0.000002	0.996
Fluoxetine	1	0.320	0.263	0.417	0.129	0.251	0.000012	0.998
	21	0.275	0.242	0.338	0.102	0.375	0.000009	0.998
Lamotrigine	1	0.411	0.531	0.406	0.256	0.172	0.000023	0.993
	21	0.329	0.383	0.398	0.213	0.261	0.000019	0.992
Venlafaxine	1	0.120	0.032	0.224	0.0407	0.644	0.000004	0.997
	21	0.098	0.016	0.218	0.0108	0.672	0.000001	0.996

*It should be noted that bupropion and duloxetine did not consider bound-residue fraction data to calculate the total concentration due to the significant loss during the alkaline hydrolysis.

Table S6. The ratio of desorbed fraction of nine psychotic drugs after 10 h methanol extraction the desorbed fraction from all extraction times at sampling time of day 1 and day 21.

Compound	Day	F_{24h}/F_r
Amitriptyline	1	0.78 ± 0.19
	21	0.75 ± 0.15
Bupropion	1	0.93 ± 0.15
	21	0.82 ± 0.18
Carbamazepine	1	0.93 ± 0.20
	21	0.87 ± 0.20
Citalopram	1	0.92 ± 0.17
	21	0.77 ± 0.17
Clozapine	1	0.81 ± 0.20
	21	0.88 ± 0.21
Duloxetine	1	0.89 ± 0.21
	21	0.80 ± 0.20
Fluoxetine	1	0.77 ± 0.20
	21	0.92 ± 0.18
Lamotrigine	1	0.90 ± 0.21
	21	0.82 ± 0.20
Venlafaxine	1	0.86 ± 0.15
	21	0.82 ± 0.17

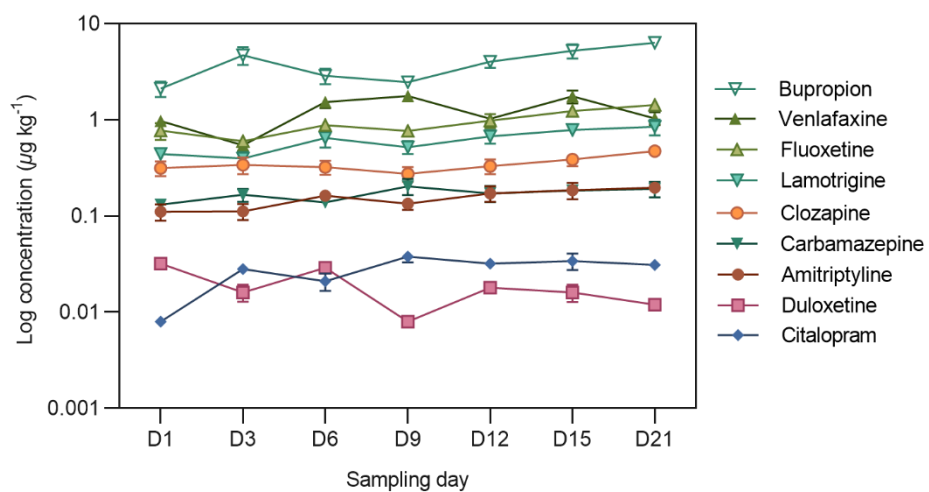


Figure S9. Logarithm-transformed concentration of nine psychotic drugs in sediment extracted for stable-desorbing fraction after the consecutive extraction for fats-desorbing fraction at each DGT deployment time. The concentration data is shown in Table S8.

Table S7. The concentration ($\mu\text{g kg}^{-1}$) of nine psychotic drugs with standard deviation from triplicate samples in sediment extracted for stable-desorbing fraction after the consecutive extraction for fast-desorbing fraction at each DGT deployment time.

Compound	D1	D3	D6	D9	D12	D15	D21
Amitriptyline	0.11±0.02	0.11±0.01	0.16±0.03	0.13±0.03	0.17±0.03	0.19±0.04	0.20±0.03
Bupropion	2.12±0.44	4.71±0.48	2.88±0.51	2.46±0.47	4.03±0.42	5.23±0.88	6.32±0.73
Carbamazepine	0.13±0.02	0.17±0.03	0.14±0.03	0.20±0.04	0.17±0.03	0.18±0.02	0.19±0.03
Citalopram	0.01±0.001	0.03±0.01	0.02±0.004	0.04±0.01	0.03±0.004	0.03±0.01	0.03±0.01
Clozapine	0.32±0.04	0.34±0.05	0.32±0.04	0.27±0.03	0.33±0.04	0.39±0.06	0.47±0.06
Duloxetine	0.03±0.01	0.02±0.002	0.03±0.01	0.01±0.001	0.02±0.002	0.02±0.003	0.01±0.001
Fluoxetine	0.77±0.08	0.60±0.08	0.88±0.16	0.77±0.09	0.98±0.21	1.23±0.14	1.43±0.28
Lamotrigine	0.44±0.05	0.40±0.05	0.65±0.13	0.52±0.06	0.68±0.12	0.79±0.10	0.85±0.16
Venlafaxine	0.98±0.13	0.54±0.07	1.53±0.24	1.77±0.34	1.03±0.15	1.75±0.26	1.04±0.15

Table S8. The concentration ($\mu\text{g kg}^{-1}$) of non-degraded psychotic drugs with standard deviation from triplicate samples in hydrolyzed sediment for bound-residue fraction at each DGT deployment time.

Compound	D1	D3	D6	D9	D12	D15	D21
Amitriptyline	0.83±0.09	1.04±0.13	1.85±0.26	1.92±0.25	2.82±2.82	2.94±0.34	3.12±0.43
Carbamazepine	0.18±0.02	0.36±0.05	0.35±0.05	0.58±0.07	0.65±0.09	0.78±0.08	0.91±0.14
Citalopram	0.01±0.001	0.02±0.003	0.01±0.002	0.03±0.003	0.06±0.01	0.04±0.01	0.02±0.003
Clozapine	1.13±0.13	0.43±0.06	0.30±0.03	0.34±0.05	0.47±0.07	0.32±0.04	0.37±0.04
Fluoxetine	0.41±0.06	0.28±0.03	0.49±0.07	0.31±0.03	0.46±0.07	0.41±0.05	0.32±0.04
Lamotrigine	0.67±0.10	1.09±0.16	1.37±0.22	2.15±0.31	2.16±0.28	3.45±0.44	3.98±0.57
Venlafaxine	0.98±0.14	1.17±0.17	1.32±0.17	1.58±0.16	2.60±0.41	3.82±0.49	4.11±0.47

Table S9. The concentration ($\mu\text{g kg}^{-1}$) of psychotic drugs in the three fractions in sampled sediments at individual time.

Compound	Fraction	1 d	3 d	6 d	9 d	12 d	15 d	21 d
Amitriptyline	Stable	0.11	0.11	0.16	0.13	0.17	0.19	0.20
	Bound	0.83	1.04	1.85	1.92	2.82	2.94	3.12
	Labile	0.42	0.49	0.78	0.76	0.79	0.73	0.68
	Total	1.37	1.64	2.80	2.82	3.78	3.86	4.00
Bupropion	Stable	2.12	4.71	2.88	2.46	4.03	5.23	6.32
	Bound	NA						
	Labile	0.78	1.65	0.91	0.58	0.71	0.85	0.94
	Total	2.91	6.36	3.79	3.04	4.74	6.08	7.27
Carbamazepine	Stable	0.13	0.17	0.14	0.20	0.17	0.18	0.19
	Bound	0.18	0.36	0.35	0.58	0.65	0.78	0.91
	Labile	0.15	0.24	0.19	0.26	0.22	0.18	0.18
	Total	0.46	0.76	0.68	1.05	1.04	1.15	1.28
Citalopram	Stable	0.01	0.03	0.02	0.04	0.03	0.03	0.03
	Bound	0.01	0.02	0.01	0.03	0.06	0.04	0.02
	Labile	0.004	0.02	0.01	0.01	0.02	0.01	0.01
	Total	0.02	0.07	0.04	0.08	0.11	0.09	0.06
Clozapine	Stable	0.32	0.34	0.32	0.27	0.33	0.39	0.47
	Bound	1.13	0.43	0.30	0.34	0.47	0.32	0.37
	Labile	0.38	0.19	0.12	0.10	0.12	0.10	0.10
	Total	1.83	0.97	0.75	0.71	0.92	0.80	0.94
Duloxetine	Stable	0.03	0.02	0.03	0.01	0.02	0.02	0.01
	Bound	NA						
	Labile	0.006	0.002	0.003	0.001	0.001	0.001	0.0004
	Total	0.04	0.02	0.03	0.01	0.02	0.02	0.01
Fluoxetine	Stable	0.77	0.60	0.88	0.77	0.98	1.23	1.43
	Bound	0.41	0.28	0.49	0.31	0.47	0.41	0.32
	Labile	0.42	0.28	0.36	0.22	0.26	0.27	0.24
	Total	1.60	1.16	1.73	1.29	1.72	1.91	1.99
Lamotrigine	Stable	0.44	0.40	0.65	0.52	0.68	0.79	0.85
	Bound	0.67	1.09	1.37	2.15	2.16	3.45	3.98
	Labile	0.50	0.61	0.78	0.89	0.90	1.27	1.28
	Total	1.61	2.09	2.80	3.56	3.73	5.50	6.11
Venlafaxine	Stable	0.98	0.54	1.53	1.77	1.03	1.75	1.04
	Bound	0.88	1.17	1.32	1.53	2.60	3.82	4.11
	Labile	0.28	0.23	0.32	0.36	0.32	0.49	0.36
	Total	2.13	1.94	3.17	3.65	3.95	6.07	5.51

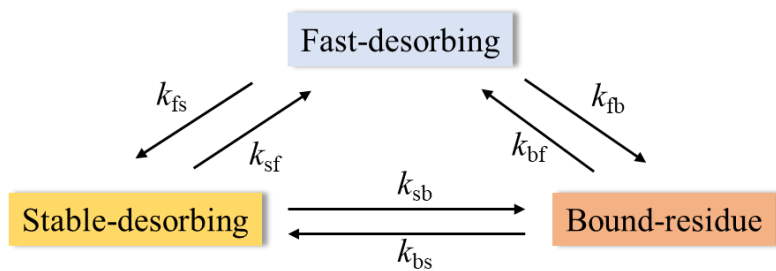


Figure S10. Illustration of transfer model of antipsychotic drug fractions in sediment.

Section S9. The computation processes of fraction transfer modeling.

The first order difference method was used to differentiate the model:

$$\frac{C_{labile}^{i+1} - C_{labile}^i}{\tau} = -k_{fs} C_{labile}^i - k_{fb} C_{labile}^i + k_{sf} C_{stable}^i + k_{bf} C_{bound}^i \quad (S15)$$

$$\frac{C_{stable}^{i+1} - C_{stable}^i}{\tau} = -k_{sf} C_{stable}^i - k_{sb} C_{stable}^i + k_{fs} C_{labile}^i + k_{bs} C_{bound}^i \quad (S16)$$

$$\frac{C_{bound}^{i+1} - C_{bound}^i}{\tau} = -k_{bf} C_{bound}^i - k_{bs} C_{bound}^i + k_{fb} C_{labile}^i + k_{sb} C_{stable}^i \quad (S17)$$

Rate coefficient k was estimated by Genetic algorithm using the results from Table S10. The minimizations of the residual errors between modelled and measured psychotic drugs concentrations was set as the fitness function:

$$\min fit(\gamma) = \sum_i (C_{cal}(t_i, \gamma) - C_{obs}(t_i, \hat{\gamma}))^2 \quad (S18)$$

$C_{cal}(t_i, \gamma)$ and $C_{obs}(t_i, \hat{\gamma})$: the modelled and measure concentrations. γ : the parameters need to estimate. τ was set as 0.2 day to run the model.

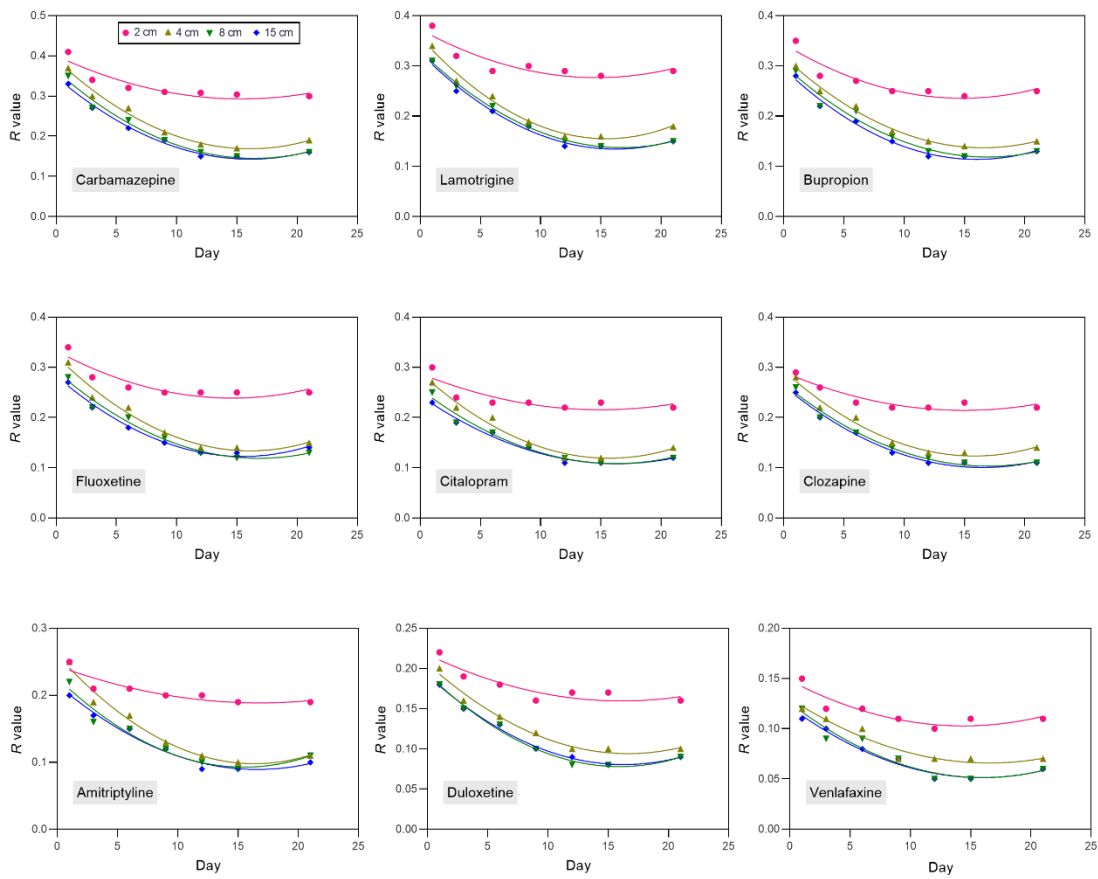


Figure S11. *R* values calculated from different depths in sediments plotted with sampling time.

References

- Cornelissen, G., Noort, P.C.M.v. and Govers, H.A.J. 1997. Desorption kinetics of chlorobenzenes, polycyclic aromatic hydrocarbons, and polychlorinated biphenyls: Sediment extraction with Tenax® and effects of contact time and solute hydrophobicity. *Environmental Toxicology and Chemistry* 16, 1351-1357.
- Crank, J. (1979) *The mathematics of diffusion*, Oxford university press.
- Cussler, E.L. (2009) *Diffusion: mass transfer in fluid systems*, Cambridge university press.
- Ganser, G.H. and Hewett, P. 2010. An Accurate Substitution Method for Analyzing Censored Data. *Journal of Occupational and Environmental Hygiene* 7(4), 233-244.
- Harper, M.P., Davison, W., Zhang, H. and Tych, W. 1998. Kinetics of metal exchange between solids and solutions in sediments and soils interpreted from DGT measured fluxes. *Geochimica et Cosmochimica Acta* 62(16), 2757-2770.
- Pignatello, J.J. 1990. Slowly reversible sorption of aliphatic halocarbons in soils. II. Mechanistic aspects. *Environmental Toxicology and Chemistry* 9(9), 1117-1126.
- Schwarzenbach, R.P., Gschwend, P.M. and Imboden, D.M. (2017) *Environmental organic chemistry*, Wiley-Interscience, New Jersey, USA.
- Sherwood, C.R., Drake, D.E., Wiberg, P.L. and Wheatcroft, R.A. 2002. Prediction of the fate of p,p'-DDE in sediment on the Palos Verdes shelf, California, USA. *Continental Shelf Research* 22(6), 1025-1058.
- Wang, X.-C., Zhang, Y.-X. and Chen, R.F. 2001. Distribution and Partitioning of Polycyclic Aromatic Hydrocarbons (PAHs) in Different Size Fractions in Sediments from Boston Harbor, United States. *Marine Pollution Bulletin* 42(11), 1139-1149.

Yuan-Hui, L. and Gregory, S. 1974. Diffusion of ions in sea water and in deep-sea sediments.

Geochimica et Cosmochimica Acta 38(5), 703-714.

Zhang, H., Davison, W., Tye, A.M., Crout, N.M.J. and Young, S.D. 2006. Kinetics of zinc

and cadmium release in freshly contaminated soils. *Environmental Toxicology and*

Chemistry 25(3), 664-670.